JOINT EUROPEAN TORUS

JET–P(92)80

A.S. Kaye
and JET Team

Progress in ICRH and Lower Hybrid Launcher Development

Progress in ICRH and Lower Hybrid Launcher Development

A.S. Kaye and JET Team*

JET-Joint Undertaking, Culham Science Centre, OX14 3DB, Abingdon, UK

** See Annex*

Preprint of an Invited Paper presented to the Europhysical Topical Conference on Radio Frequency Heating and Current Drive of Fusion Devices (Brussels, July 1992) and to be submitted for publication in Plasma Physics and Controlled Fusion

PROGRESS IN ICRH AND LOWER HYBRID LAUNCHER DEVELOPMENT

A S Kaye

JET Joint Undertaking, Abingdon, Oxon, OX14 3EA, UK

ABSTRACT

Radio frequency methods of heating and non-inductive current drive have become well established and are likely to be part of any next-step Tokamak programme. This paper reviews the present state of development of antennae for ion cyclotron heating and recent developments to enhance the effectiveness of fast wave current drive systems. The performance achieved by present systems enables the provision of an ICRH system for next step devices within the existing technology limits.

The main Lower Hybrid current drive systems are also reviewed. Present operating limits suggest that the design power density at the grill in large multijunction launchers must be somewhat reduced due to peaking of the electric field. The resulting launcher for a next step machine based on present technology is a large and highly complex device. Development of recent proposals such as the rod array or the hyperguide, in parallel with necessary improvements in the current drive efficiency would make Lower Hybrid a more attractive method of non-inductive current drive for next step machines.

KEYWORDS

Tokamak, Radio Frequency, ICRH, LHCD, Heating, Current Drive, Antenna, Microwave

INTRODUCTION

Over the past decade, radio frequency systems have become established as an important part of the fusion programme [GORMEZANO, 1991]. Ion cyclotron heating systems have made particular progress in recent years, with the improved understanding of impurity production mechanisms leading to the generation of RF only H-modes [STEINMETZ et al, 1990; MATSUMOTO et al, 1990; TUBBING et al, 1991] as well as many other heating scenarios. High power systems are now in operation at JET [JACQUINOT, 1992], TFTR [HOSEA et al, 1990] and JT-60U [KIMURA et al, 1992], and many smaller machines, and are being planned for next step machines. Fast wave current drive is emerging as an alternative means of non-inductive current drive, although the efficiencies achieved to date are low if the fast wave is used alone.

Lower Hybrid electron heating has been well established for some years. The main thrust in recent years has been on current drive systems. Multi-megawatt systems are operational at JT-60U [IDE et al,1992], Tore Supra [MOREAU et al, 1992] and JET [GORMEZANO et al, 1991]. Current drive efficiencies are the highest achieved of any method of non-inductive current drive.The discovery of synergistic effects with ion cyclotron heating [GORMEZANO et al, 1991; BHATNAGAR, JACQUINOT et al, 1991] has raised the potential for significant further increases in efficiency. Such improvements are a critical prerequisite for the design of steady state reactor systems [WILHELM, 1988; WEGROWE et al, 1991; REBUT, 1992].

This paper reviews the design of existing ICRF and LHCD systems, and discusses recent developments and proposals for alternative systems to those currently in use. The requirements for next step machines and conceptual designs of antennae and launchers for such machines are considered.

1. DEVELOPMENT OF ICRH SYSTEMS

1.1 Background

High power ICRF antennae are presently operating on many fusion machines around the world, including JET [KAYE et al, 1992], TFTR [HOSEA, 1991] and JT-60U [FUJII, 1990]. Table 1 lists the larger of these systems and their main parameters. Installed powers up to 32 MW, coupled power up to 22 MW, coupled power density at the antenna up to 16 MW/m^2 have been achieved with presently operating systems. These systems all have the same basic design. Co-axial transmission lines are used to feed power from tetrode sources via ceramic vacuum windows to antennae mounted at the torus wall.

Table 1. Design parameters for some existing ICRH systems. Figures in brackets indicate imminent upgrades.

	Generator Power MW	Frequency MHz	No Antennae
Asdex-U	8	30 - 120	4
D111-D	2	30 - 90	2
JET	32	23 - 57	8
JT-60-U	6(9.5	108 - 132	2
TEXTOR	3	25 - 40	2
TFTR	10(14)	47(40-80)	2(4)
Tore Supra	12	35 - 80	3

Current straps in the antenna aligned in the poloidal direction are used to excite the fast magnetosonic wave which propagates radially into the plasma. All metal slotted Faraday screens are used to isolate the high voltage on the strap from the plasma.

Present antennae fall into two groups. Those at JET, TEXTOR, ASDEX Upgrade are installed into the torus through a main port and mounted onto the torus wall in the gap between the wall and the plasma. Incoming transmission lines are inserted through small ports onto the back of the antennae. The JET antennae and transmission lines are illustrated in Fig 1 for example. This type of construction enables the use of antennae of large frontal area and low power density at the screen and requires modest opening through the vessel, which reduces the neutron flux in the lines. The restricted depth can limit the coupling resistance.

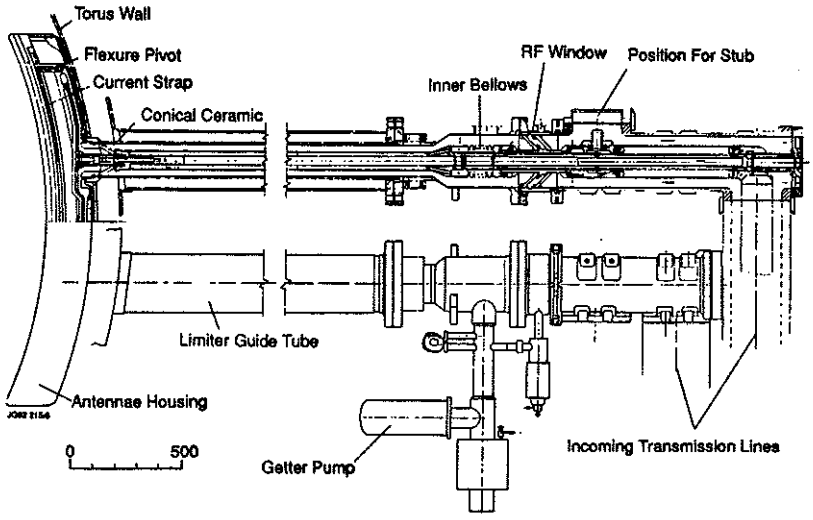

Fig 1. A vertical section through the JET antenna.

The alternative approach is the 'plug' antenna as used on TFTR,Tore Supra, JT-60. In this case, the antenna and transmission lines are prepared as a complete self-contained assembly which is inserted into main access ports. The antenna of Tore Supra is shown in Fig 2 as an example. This approach restricts the frontal area of the antenna and imposes high power density. The coupling resistance benefits from the generally larger depth available in such designs which compensates for the reduced frontal area. The coupling may now be limited by the width rather than the depth, due to image currents in the side walls.

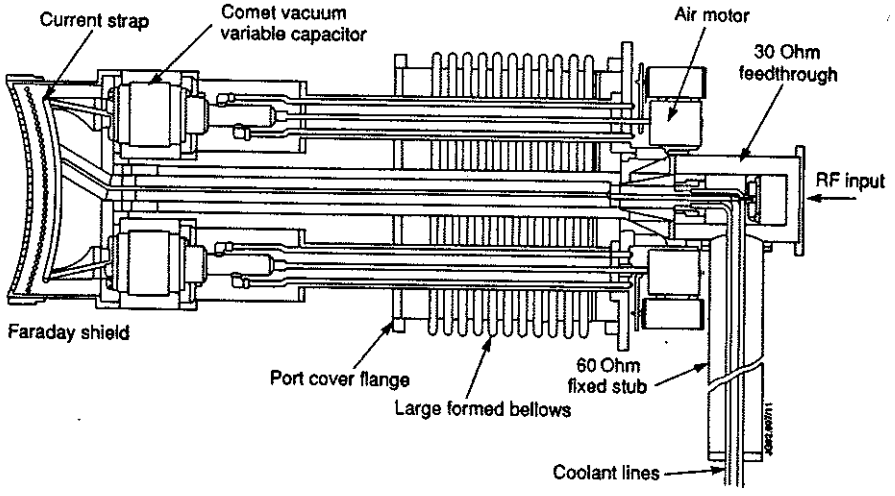

Fig 2. A vertical section through the Tore Supra antenna

The performance achieved to date by the various systems is summarised in Table 2. ASDEX upgrade and JT-60U are presently bringing their systems on-line. Operating systems have achieved coupled powers up to 22 MW (JET), whilst all of the machines listed are operating in the multi-megawatt range. The pulse data for the 22 MW pulse at JET is shown in Fig 3. Coupled energies range up to nearly 200 MJ on JET. The design pulse durations range from a few seconds to effectively continuous in the case of Tore Supra, where all parts are water cooled. The maximum pulse length is 60 seconds on Tore Supra and JET, in the latter case by operating pairs of antennae for 20 seconds each in sequence.

Table 2. Performance achieved on present systems.

	Coupled Power MW	Energy MJ
Asdex-U		Commissioning
D111-D	1.6	3
JET	22	180
JT-60	3.1	
JT-60-U	1.5	
TEXTOR	3.6	2
TFTR	7	14
Tore Supra	4	60

The performance of individual antennae is summarised in Table 3. The power per antenna ranges up to 5 MW (TFTR). The power density at the screens varies from 4 MW/m^2 on JET, to 10-16 MW/m^2 on the plug type antennae of TFTR,Tore Supra and JT-60. The power density averaged over the direct vessel access is much increased to values in excess of 100 MW/m^2 except for plug-type antenna, for which it is essentially unchanged.

Table 3. Performance achieved on present ICRH antennae. The electric fields are estimates of the peak field parallel and perpendicular to the magnetic field. Breakdown normally only occurrs parallel to the magnetic field.

	Screen Area m2	Power/ Antenna MW	Power Density MW/m^2	Peak Volt kV	Peak E-field kV/mm Par	Perp
Asdex-U	0.72	(2)	(2.5)			
D111-D	0.21	1.7	8	30		
JET	0.9	3.2	3.5	30	2	3
JT-60	0.19	3	16			
JT-60-U	0.63	3				
TEXTOR	0.42	2.2	5			
TFTR(PPPL)	0.65	5	10	40	3	4
Tore Supra	0.28	3.6	12	35	1.5	

Perhaps of more significance in determining the limits to performance of the antenna is the electric field strength. The maximum operating voltage of a system is generally not sharply defined and depends on such factors as conditioning,temperature. Nonetheless, some data are given in Table 3 for the maximum sustainable voltage on several systems. These are in the range 30-40 kV. The corresponding peak electric field is even less well defined as it depends on the fine detail of the design, notably the curvature of the surface. Estimated values parallel to the magnetic field for TFTR and Tore Supra are also given in Table 3, together with the peak value at the conical ceramic in JET. Substantially higher fields are sustainable across the magnetic field. Estimated values are also given in Table 3. This field appears between the strap and the screen in each case. Arcing here is rare and the values listed may not represent upper limits. Design within these values, say 3 kV/mm, should be safe.

It appears from Table 3 that the most consistent limiting parameter is the voltage. It may however be expected that the electric field is the real limitation. Design values of 1.5 kV/mm parallel to the magnetic field and 3 kV/mm perpendicular to the magnetic field are suggested by this data.

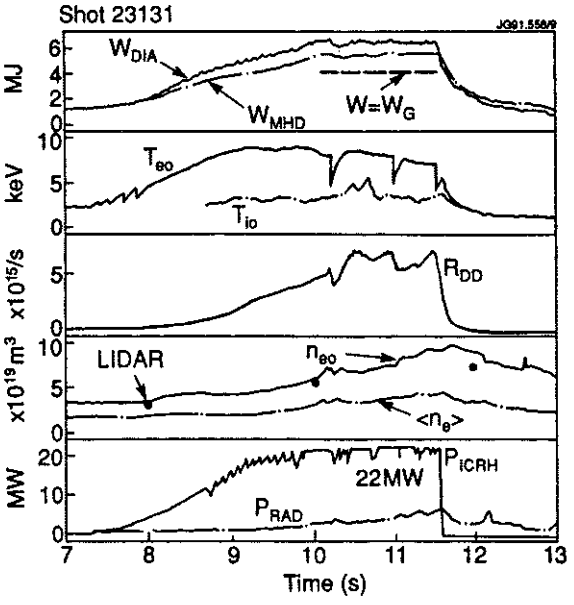

Fig 3. 22 MW coupled ICRH power at JET.

Whilst the principles of all systems are similar, there are many variations in the detail of the designs. The details of these systems are reviewed below.

1.2 Vacuum Windows

Many designs of vacuum windows for co-axial lines capable of operatimg routinely at megawatts of coupled power have been designed and manufactured [BAITY et el, 1986; KAYE et al, 1987; FUJII et al, 1991]. These windows are (with the exception of Tore Supra and TFTR/ORNL designs) located between the antenna and the tuning stubs, and therefore carry a high circulating power. Total forward power is tens of megawatts. These windows mainly utilise metallised alumina ceramic vacuum brazed to the inner and outer conductors, although compression seals are used successfuly on the ASDEX [WEDLER, 1992] and Tore Supra windows. The ceramic is usually conical or cylindrical in order to reduce the field enhancement due to the high dielectric constant of alumina, and the conductors are contoured to minimise the electric field and maintain near constant impedance through the window. RF peak voltages up to 70 kV have been obtained and 50 kV is common in both 30 ohm and 50 ohm designs. In a 9 inch/30 ohm line, this corresponds to a forward power of 60 MW per window, or 2GW/m^2, with a peak electric field of order 2 kV/mm.

The windows from ORNL use water cooling; inertial cooling is sufficient for most current applications at duty cycles below 1:10. An assessment of the requirements for next step devices [BROWN, 1992] shows that dielectric losses leading to thermal stresses limit the steady state power. However, edge cooling is adequate for loss tangents typical of present materials. Neutron irradiation of the ceramic leads to an increase in dielectric losses which limits the total fluence acceptable to about 10^{21}/m^2. Catastrophic failure has recently been shown to occur under neutron irradiation at elevated temperature (300-500 C) in the presence of DC or RF electric fields of the magnitude required in these windows [HODGSON, 1991]. This may limit also the maximum temperature in the ceramic.

A substantial reduction in thermal stress can be achieved using beryllium oxide ceramic. This is routinely done with high power microwave windows. The effects of neutrons on the properties of beryllia have only been superficially explored.

A double window, using two closely spaced ceramics with a pumped interspace, is used on JET for security of tritium confinement [KAYE et al, 1987]. It is anticipated that a similar design will be required on next step devices.

The main hazard for these windows is the occurrence of arcs at the window. Microwave systems routinely use optical detectors for protection. This has only been applied to the ICRF system on JT-60U to date [FUJII et al, 1990]. Instead, reflected power alarms are used to trip the generators. It is however preferred to locate the window at a voltage minimum. Arcs at this position are difficult to detect as they result in minor change in input impedance. As the matching systems become evermore sophisticated, the possibility of matching onto such an arc enhances the need for an independent arc detection system.

1.3 Vacuum Transmission Lines

Existing ICRF systems all use a length of co-axial line inside the vacuum system to connect the window to the antenna. This line will be referred to as the vacuum transmission line (VTL). Present systems use 25, 30 and 50 ohm lines. The VTL may contain additional ceramic supports for the inner conductor (see for example Figs 1-2). The line diameter is often limited by the available space and is typically in the range 60 to 120 mm.

The design of this line is critical to the ultimate performance of the system; many systems are limited by breakdown in the line rather than the antenna. For example, the JET line has been illustrated in Fig 1. The conical ceramic is required to support the inner conductor and current strap against disruption loads and has been designed to minimise the electric field near the ceramic. As the current strap is typically near to a quarter wavelength long, this ceramic (and its equivalent on other machines) is near to a voltage maximum. Arcing parallel to the magnetic field at this ceramic is the clear limit to the performance of the JET antennae. The resulting deposition of sputtered metal on the ceramic, if this arc is not detected soon enough, ultimately leads to failure of the antenna.

The estimated maximum electric field parallel to the magnetic field near the first voltage maximum for various machines has been tabulated in Table 3 (in the case of Tore Supra, this occurs at the capacitative terminations to the strap). The limiting value varies from 1.2 to 3 kV/mm. This spread would be consistent with the errors in this estimation arising from uncertainties in electrical length of the strap and field enhancements in the VTL.

It is noted that the limiting voltage on the torus at JET is about a factor 2 below that which can be obtained in the test bed. The reasons for this degradation on the torus are not clear, but may arise for example from the magnetic field, the ionising radiation, the presence of highly excited neutral particles, or transient increases in line voltage due to the varying load or cross coupling.

In next step devices, it is strongly preferred and may be essential to avoid the use of ceramic supports close to the plasma.

Current carrying surfaces of the VTL are coated with high conductivity metal to a thickness of several skin depths to minimise the RF losses. Many systems use copper. Tests at JET [KAYE et al, 1987] showed that silver could be conditioned more easily than copper and all RF surfaces are silver plated. Similar results were found at JET at microwave frequencies [KAYE et al, 1988]. Recently, ASDEX have found that gold is preferable to silver for conditioning [WEDLER et al, 1992] and JET have successfully tested an antenna model with nickel plating [KAYE et al, 1992]. The losses are a factor 2-3 higher with nickel but this is not critical in systems which must be actively cooled anyway. The use of silver is difficult in next step devices due to the disproportionate production of active waste [BUTTERWORTH, 1988]. The application of electroplated coatings having the conductivity and adhesion required is a diffficult technology which few firms have mastered. Baking of the components in vacuum is an effective check of the adhesion.

The pressure in the VTL is also a critical parameter. Arcing is an increasingly severe problem above 10^{-4} mbar. Auxiliary vacuum systems are provided on several machines to maintain this vacuum. Active metal getter pumps have been successfully used on JET [WALKER et al, 1988], and cryopumps on ASDEX Upgrade [WEDLER et al, 1992] for this purpose.

1.4 Housing and Current Straps

Existing systems utilise a range of layouts of the current straps. In general, the current straps have short circuit terminations within the housing. Such straps tend to be simple to manufacture, robust and broadband.

Antennae at TFTR and Tore Supra have internal capacitative termination. The Tore Supra antenna has been shown in Fig 2. With these capacitors, by connecting the strap off-centre as seen in Fig 2, the VTL is matched to the strap at the design coupling resistance and sees only a low VSWR and thus low peak voltage and losses. Disadvantages of this approach are the difficulty in achieving the required rating on the capacitors, the requirement to use ceramics close to the plasma, and the requirement to adjust the capacitors to accommodate changes in the loading resistance. On the other hand, the match is tolerant of small changes in coupling.

Connection of two or more poloidally displaced straps in parallel to the one VTL as in JET, ASDEX and JT-60U reduces the strap impedance to better match the VTL and also allows increased coupling per VTL if the resulting straps are near one quarter wavelength in length. Parallel connection of toroidally displaced straps has a similar benefit but does not allow control of the spectrum. An extension of this to many parallel straps has been proposed on D III-D [MOELLER et al, 1992], and Wendelstein [CATTANEI et al, 1989].

As with the VTL, the current strap is conventionally coated with high conductivity metal to reduce losses. The increasing use of open screen structures (or possibly no screens) exposes the strap to the plasma. The migration of metals between screen and strap has been investigated at ASDEX [BEHRISCH et al, 1987]. Whilst no evidence has been found of impurities from the strap entering the plasma, next step machines may require armour on the straps to protect against the heat pulse during disruptions.

The antenna housing is typically an open-fronted box which serves two purposes. It is a mechanical structure on which to mount the current strap, screen and VTL. It is also the return conductor for the RF current. These functions are traditionally combined.

The mechanical support function is strongly dependent on the machine. On many machines, the provision of an ICRF system has been a late development and no provision was made in the original structure. These include TFTR and JET. TFTR overcame this problem by designing plug-in antennae to fit into the main horizontal ports. A similar approach is used on JT-60U and Tore Supra. These antennae have of necessity to operate at high coupled power density (see Table 3), typically 10 MW/m^2. The surrounding torus structure partly screens the antenna from disruption forces.

Other projects have chosen instead to locate the antennae in the gap between the plasma and the torus wall, notably JET,Textor,ASDEX Upgrade. These antennae are relatively large in frontal area and operate at low power density, 2-4 MW/m^2. The depth of these antennae is however constrained and the coupling is consequently reduced. Some screening from eddy currents is provided by the torus structure, which is used to support the antenna. An extreme case is the new A2 antenna on JET which projects up to 1m into the torus. Whilst this allows increased depth and thus coupling, this antenna is exposed to severe eddy currents. The resulting forces are supported only by the torus wall and minimisation of these forces has driven the design. The resulting housing is fabricated from 0.8 mm sheet metal, and other novel features have been required to produce an acceptable design [LOBEL et al,1990].

Next step machines are likely to include provision for ICRF from the outset. This enables optimisation of the antenna, its location and mechanical support free of many of the constraints of existing systems. Full advantage should be taken of this opportunity.

The role of the antenna housing as a return conductor has become increasingly important with the development of fast wave current drive (FWCD) scenarios. The launched spectrum depends on the return current as well as that in the straps. In particuler, image currents in the side walls can substantially degrade the spectrum. As the housing depth is increased on larger machines to improve the coupling, so these sidewall image currents increase. This can limit the improvement in coupling.

These problems are addressed by slotting the sidewalls of the housing (and septum if used), for example on TFTR and JET A2 antennae. In JET, the slot depth is 100 mm. These slots improve the directivity but compound the problem of disruption forces on the screens, and also allow neutral particles access to the antenna from the sides.

1.5 Faraday Screens

ICRF antennae have been fitted with Faraday screens since the earliest experiments on the C-stellerator [YOSHIKAWA et al, 1965]. The all-metal slotted screen was developed on TFR in 1978 [JACQUINOT, 1978] and co-incided with major improvements in the performance of ICRF heating systems. The tilted screen, with elements inclined to be parallel to the magnetic field was introduced in JET in 1984 [ARBEZ et al, 1984] as an attempt to control the release of impurities which had become a major problem with ICRF heating. Early metal screens allowed no line-of-sight through the screen by using overlapping elements of a variety of cross-section. The longer pulse duration devices were obliged to produce directly water-cooled screens due to the high losses of these elements. Experiments in the mid 1980's [NOTERDAEME et al, 1986] showed that open screens having a clear line-of-sight also performed well. This enabled considerable simplification of the design of the screen, and in particular, a move away from directly cooled screens on present generation machines. Recently, an antenna on TEXTOR has been operated without any Faraday screen but with careful attention to the side protection [VAN NIEUWENHOVE et al, 1991]. The good results obtained at TEXTOR have also been found subsequently at PHAEDRUS [HERSKOWITZ et al, 1992] in combination with boron carbide coated side protection. Current experiments at DIII-D look less promising [PINSKER, 1992].

The Faraday screens on existing antennae are all of similar conceptual design. A series of parallel metal rods approximately parallel to the magnetic field are mounted between the current strap and the plasma. These rods are electrically connected to each other and the housing at both ends. This connection may be direct, or via resistors [LOBEL et al, 1990] or capacitors [NOTERDAEME et al, 1992], these latter being used to reduce disruption induced eddy currents.

This structure is transparent to RF electric fields polarised normal to the screen elements. It is this component which couples to the fast wave. The component parallel to the screen elements is reflected from the screen. This has the effect of selectively exciting the fast wave whilst suppressing the slow wave. This is particularly the case if the screen elements are tilted to be parallel to the magnetic field rather than horizontal, and is the original motivation for introducing the tilted screen.

The conducting screen elements force the RF field to be compressed through the gaps between elements. The associated eddy currents in the elements lead to significant RF losses and heating of the screen. The magnitude of these losses depends mainly on the ratio of the gap to the element width and the surface conductivity of the rods. For long pulse/steady state operation it is essential to directly cool the rods. Some systems have used direct water cooling (JET nickel screens, ASDEX, JT-60, TFTR/ORNL version, Tore Supra). However, the steady move to more open screen structures has much reduced the RF losses in the elements and enabled the design of screens relying only on end cooling of the elements. JET and ASDEX

Upgrade have now moved to end cooling of the elements, which is a viable solution for present machines of limited duty cycle and pulse length and avoids the severe complication and reliability problems associated with direct water cooling.

End cooling of the screen elements is achieved using multiple foil flexure pivots to establish good thermal contact to the end manifold whilst accomodating differential thermal expansion. Suitable element materials are beryllium (JET) or molybdenum (ASDEX Upgrade), or possibly copper alloys.

Direct cooled or radiation cooled elements can use nickel alloys (TFTR,DIII-D,JT-60U,Tore Supra) or pure nickel (JET). The use of low conductivity nickel alloys requires coating with copper or equivalent to reduce losses. This in turn is coated with refractory material for protection. Materials which have ben used include TiC (ASDEX, JT-60), TiCN (TFTR/PPPL, DIII-D), graphite (TFTR/ORNL), thin carbon (JT-60U) and boron carbide (Tore Supra,DIII-D). In general, these coatings have performed well apart from the graphite. This took the form of tiles vacuum brazed to the elements. These are very lossy and the manufacturing technique severely restricts the shape of the elements. The recent designs from ORNL for Tore Supra and DIII-D use plasma sprayed boron carbide for which initial results are very encouraging [BEAUMONT,1992]. This material has low z, very high melting point, and semi-conductor electrical properties. The skin depth at ICRF frequencies is typically several millimetres, enabling low-loss layers of a few tenths of a millimetre to be applied. This compares to hundredths of a millimetre for titanium carbide.

1.6 RF Specific Impurity Production

Impurity production during ICRF heating has been a persistent problem since the earliest experiments. Over the past decade, many experiments have been carried out to try to understand the mechanisms involved. These have resulted in the development of a model based on RF sheath rectification, enhanced by direct RF absorption in the edge plasma under conditions of low absorption, which appears to correlate well with the bulk of the experimental data. The details of this model and its evolution have been recently reviewed in detail [NOTERDAEME, 1991].

The dominant mechanism is rectification of the RF field at the sheath on the screen or side protection [PERKINS, 1989; CHODURA et al, 1989; D'IPPOLITO et al, 1990; MYRA et al, 1990; BURES et al, 1991; D'IPPOLITO et al, 1991]. This leads to the appearance of DC electric fields along the magnetic field at the sheath which accelerate ions into the surface. The resulting sputtering leads not only to direct impurity influx, but also to re-ionisation of the sputtered material and self-sputtering at the surface with an associated substantial increase in yield. Radial variation in this sheath potential leads to a radial electric field and the establishment of vertical convective cells in front of the screen [JACQUINOT et al, 1991].

This mechanism depends on the existance of a closed loop formed by a magnetic surface linking the screen to surrounding features, such as the antenna side protection, the limiters or other first wall features, or linking discrete positions on the screen itself. Any net RF flux linking this loop will induce an RF voltage around the loop which will be rectified by the sheaths. This process can be inhibited and the resulting impurity influx reduced by various means, including:

- reducing the loop area to zero by tilting the screen elements to be parallel to the field.
- reducing the nett flux linkage to zero by suitable phasing of the current straps such that the flux contributions from each strap cancel (corresponding to dipole operation).
- choosing materials with low sputtering yield by hydrogen isotopes and oxygen, and low self sputtering yield, in the 0.5-1 keV energy range (for example, beryllium).
- introducing an electrical break in the external part of the loop, for example by electrically isolating the side protection tiles on the antenna.

The first three means above are consistent with a wide body of experimental evidence as summarised by Noterdaeme. The fourth approach has recently been successfully demonstrated on the PHAEDRUS experiment [MAJESKI et al, 1991]. The reactor relevance of this technique is doubtful, but it further establishes the validity of the model.

The effects of long range RF fields can also be suppressed by choosing scenarios having a high single pass damping. The development in understanding of this mechanism and the resulting changes in operation and design have resulted in RF specific impurities being reduced to negligible levels in many machines, for example, an increase in z_{eff} in JET in dipole operation of 0.001/MW. This is a critical development for ICRF heating systems and has, for example, led directly to the production of RF only H-modes. Whether this situation will continue in high power FWCD experiments with low damping per pass remains to be seen.

1.7 The Screenless Antenna

Following improved understanding of the impurity control mechanisms, an antenna has been operated without a screen on TEXTOR [VAN NIEWENHOVE et al,1991; VAN OOST et al,1992]. The antenna side protection was such that the density at the front face of the current strap was below $10^{14}/m^3$. Some initial difficulties thought to arise from local electric field concentrations, were overcome by covering one third of the antenna near the VTL connection. Subsequently, reliable operation has been achieved at power levels similar to that obtained with the screen. The production of impurities has been studied in detail. In general, the impurity levels during screenless operation are indistinguishable from those with screen apart from some modest increase in the level of iron.

Similar good results have been obtained on PHAEDRUS, where a severe impurity problem has been overcome with a combination of screenless antenna and electrically isolated side protection.

DIII-D have also been operating recently without screens on their antenna. The difficulty of maintaining a good match during perturbations in edge density has been exacerbated, and the peak operating voltage appears to be significantly reduced. It is not clear if the limitation is in the antenna rather or the matching network.

It is noted that removing the screen from an antenna, in addition to removal of the rectified sheath at the screen, will increase the phase velocity in the antenna and change the impedance of the current strap and thus the mismatch at the VTL connection. The observation that the matching conditions are little different may reflect a cancellation of these effects. The increased phase velocity reduces the electrical length of the strap which should improve the coupling. It also reduces the voltage at the VTL connection. The need to cover part of the Textor antenna, and reduced peak voltage seen at DIII-D may reflect some voltage limit? This could limit the size and power density of screenless antennae on large tokamaks.

A further concern is that removal of the screen will enhance the convective cell in front of the screen which will increase transport in the edge plasma and may be incompatible with H-mode operation. This needs further experimental evaluation.

The screen comprises a substantial part of the cost and complexity of antennae. Confirmation that reliable H-mode operation can be sustained on reactor scale systems without the screen would lead to a significant simplification of the antenna.

1.8 Fast Wave Current Drive Antennae

The recent interest in fast wave current drive has led to a re-assessment of the design of the antenna to optimise current drive efficiency. These studies have concentrated on the optimisation of the spectrum and of the matching network.

The spectrum excited by the antennae depends both on the strap current distribution and on the return currents, in particular, currents in the sidewall of the antenna. Improvements in the spectrum have been obtained, for example on DIII-D, by grouping antennae in order to obtain four straps at regular toroidal pitch. A similar array of four straps is under construction for the JET A2 antennae.

The side wall currents degrade the spectrum. The JET A2 antennae will have slotted sidewalls and septum to minimise these currents as discussed above. The resulting spectra is compared to the A1 antenna in Fig 4 [BHATNAGAR et al, 1991]. The increase in number of straps to four has led to a narrowing and peaking of the spectrum. The slotting has avoided a corresponding increase in the sidelobes. The model used for this calculation assumes no sidewall current.

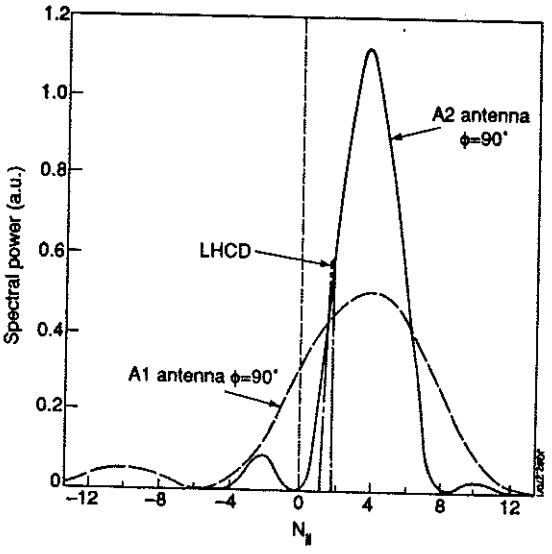

Fig 4. Computed power spectra for the JET A1 and A2 antenna arrays.

The matching of such a coupled array is the subject of detailed study. Coupling between straps with phasing other than zero or 180 degrees leads to the leading strap coupling higher power than the lagging strap for the same current. The control system must allow this. Such systems have been successfully operated at DIII-D [PINSKER et al, 1991], JET [WADE et al, 1991] and JFT2-M [SAIGUSA et al, 1991], with 90 degree phase shift between straps, and the first data on FWCD reported as a result.

The non-uniform power loading reduces the peak power capability of the system due to limiting of the most heavily loaded generator. This can be avoided by provision of an external compensating connection between the leading and lagging straps as shown in Fig 5. Such a network is being analysed by ORNL for the JET system. Initial results show that a two line compensation is effective in maintaining nearly full power capability at 90 degree phasing, as shown in Fig 6.

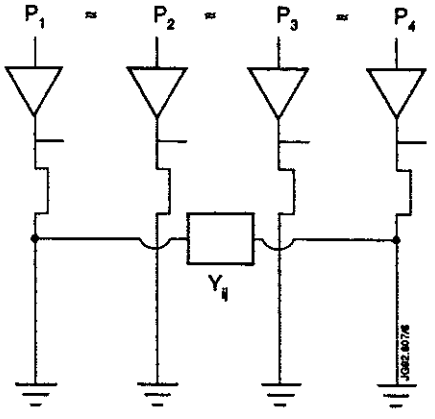

Fig 5. Schematic of the conjugate matching system for power optimisation during FWCD experiments using a 4-port network coupling lines 1 and 4.

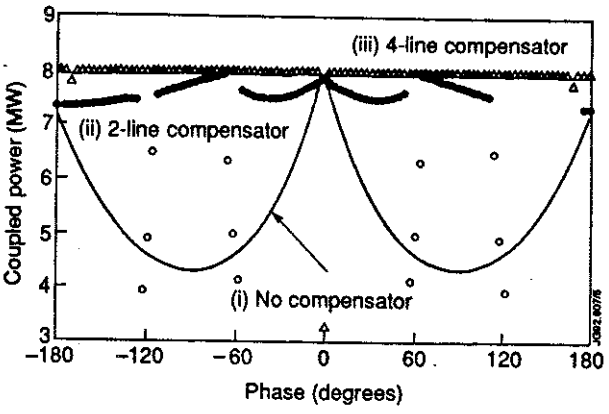

Fig 6. The computed coupled power using the conjugate matching network, with equal strap voltages and currents, and 20 ohm coupling resistance.

2. ALTERNATIVE COUPLING STRUCTURES

Whilst existing systems all utilise antennae of basically similar design, there have been proposals for alternative structures for exciting the fast wave. These include the folded waveguide first proposed by [OWENS, 1986]. One of the proposals to the ITER CDA comprised a ridged waveguide array. Many variations on travelling wave coupling structures have been considered analytically [LONGINOV, 1989]. A multiple strap array with a single feed is being considered for Wendelstein stellerator [CATTANEI et al, 1989]. Only the folded waveguide has been subject to significant development of equipment,including high power testing, and only this device will be further considered here.

The folded waveguide has been proposed for exciting the fast wave. It comprises a conventional single mode waveguide operating at ICRF frequencies, and thus of large cross-section; even at 60 MHz, the height must exceed cut-off at 2.5 m. This waveguide is terminated with a slotted short circuit and folded as illustrated in Fig 7. The outer end is terminated with a continuous short circuit and the length of the waveguide is chosen to be one half wavelength in the guide. This produces a standing wave in the waveguide and a horizontally polarised magnetic field distribution at the grill which couples effectively to the fast wave. The resulting structure is sufficiently compact to fit through the main horizontal ports on present generation machines.

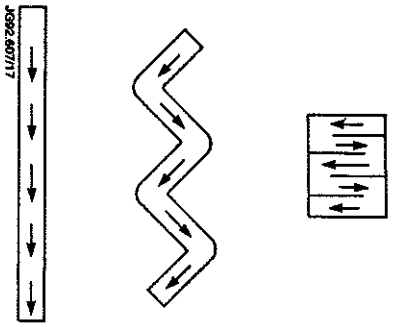

Fig 7. Principle of the folded waveguide antenna.

The major advantage potentially offerred by this approach is that the electric fields at the grill mouth are low compared to the field maximum on present antennae [CARTER et al, 1991]. This raises the possibility that substantially higher power densities may be achieved.

A test launcher of this design has been constructed at ORNL and tested on their test bed with tenuous plasma load. Initial operating experience has been highly favourable with regard to the power density achieved in comparison with conventional antennae on the same test bed [BAITY et al, 1991].

The dimensions of the folded waveguide necessitate their location in the main ports even of next step devices. This severely resticts the frontal area available when compared to conventional antennae. Only if the anticipated increase in power density is realised would this area be adequate. The dimensions also limit the frequency to the upper half of the 17-80 MHz range anticipated in the ITER CDA. This would not allow operation at 17 MHz for FWCD. Furthermore, the system is narrow band and will not allow the versatility in scenario of the conventional antenna.

This system offers a number of potential advantages. It is essential that these are demonstrated in operation in a tokamak environment before consideration for next step machines. Such demonstrations are being considered at FTU, PBX and C-MOD.

3. ICRH ANTENNAE FOR NEXT STEP MACHINES

The various operating scenarios and physics issues for an ICRF system on ITER have been considered in detail elsewhere [WEGROVE et al,1991]. Critical requirements affecting the antennae include the following:

- For heating, a total power of 50 MW at 33-66 MHz
- For current drive, 50 MW at 17 or 56 MHz
- Steady state operation
- Neutron fluence at the first wall $10^{26}/m^2$
- lifetime of 9000 burn hours
- 1000 full energy disruptions

Experience with presently operating systems would suggest that the following features should be incorporated in the design of an ICRH antenna meeting these requirements:

- The screens should be tilted, open, directly cooled and of low z material in order to minimise losses and impurities. Beryllium has given excellent performance on JET. Neutron embrittlement may be a problem. Test data suggests that this is not the case [BEESTON, 1984] at least at elevated temperature. Such data is required for the much improved grades of material now available. The heat blast during disruptions has been estimated to lead to a loss of 100 microns of material [van der LAAN et al, 1991]. Experience at JET shows a general deposition of material on the screen during plasma operation. These effects may compensate. The recent results with boron carbide begin to establish its viability as an alternative screen cladding material.

- The electric field should not exceed 1.5 kV/mm parallel or 3 kV/mm normal to the magnetic field.

Ceramic supports in the VTL are to be avoided, and the window located far from the plasma with a neutron fluence in the range 10^{20}-$10^{22}/m^2$, to be confirmed following on-going materials tests. The ceramic must be kept below typically 250 C.

The optimum poloidal location of the antenna depends on the scenario. For heating systems, location of the antenna in the main horizontal ports or in the blanket above or alonside the ports is acceptable. FWCD applications are sensitive to upshift in the $k_{//}$ spectrum [BHATNAGAR, 1990; JAEGER, 1991]. This becomes an increasing problem as the antenna are moved away from the centreline and precludes their location above the ports for the 17 MHz scenario. Their may be a regime at typically 55 MHz where location above the ports is acceptable even for FWCD [JAEGER, 1992].

An outline design of an antenna for NET taking account of these factors has been produced at JET [BROWN, 1992]. This antenna is shown in Fig 8. The characteristic features are the helical pipework forming both the screen and the housing with the minimum of welds, and the robust section of the current strap. The VTL of this design did not use ceramic supports inside the window, which was 8 m from the first wall where the neutron fluence is estimated to be $10^{20}/m^2$.

The NET design was an in-port design with remote handling capability. This severely complicates the design. The basic antenna may equally be located in the blanket. Failure analysis of the antenna shows a failure rate of 80,000 hours per antenna which is compatible with location in the blanket.

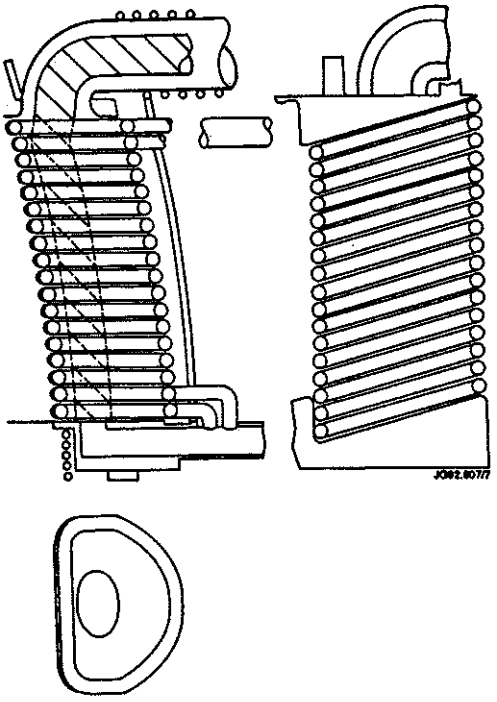

Fig 8. An outline antenna design for NET.

Location of the antennae in the blanket above the ports as illustrated in Fig 9a offers important advantages. A full circumferential ring of 96 antennae would have the properties listed in Table 4. The space occupied is of low premium in comparison with the main horizontal ports, the main issue being the loss of tritium breeding. This effect is small, typically a few percent, depending critically on whether there is adequate room behind the antenna for a breeding blanket. The power density and voltage on such an array of antennae is well inside existing technology.

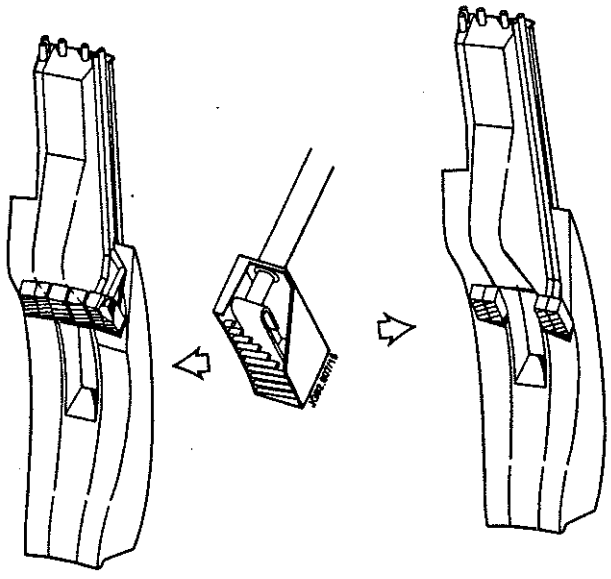

Fig 9. A schematic view of an in-blanket antenna for ITER; (a) up to 96 antennae above the ports and (b) up to 64 antennae between the ports

A FWCD system at 55 MHz comprising a double row of antenna in the blanket above the ports would suffer only a small loss of current drive efficiency compared to on-axis systems and would offer improved coupling per antenna.

Location of the antennae between the ports (Fig 9b) enables efficient FWCD operation at 17 MHz and still allows provision of 64 antennae having a unit power and power density as also listed in Table 4. This remains comfortably within the reliable operating regime of existing systems. No remote handling would be possible, but the low duty and relative lack of complication through not having a remote capability, and the redundancy in provision of antennae made possible by such a location is anticipated to be sufficient to avoid any remote handling requirement.

Table 4. Parameters of in-blanket antennae for 50 MW heating or FWCD, using a complete ring of 96 antennae above the ports or 64 antennae between ports. A reduced number of antennae may be used at proportionately higher loading and voltage per antenna.

No of antennae	96	64
Screen frontal area	30	20 m^2
Antenna frontal area	50	33 m^2
Fraction of FW area	5	3.5 %
Volume of antenna	25	16 m^3
Volume of VTL	10	7 m^3

Fraction of blanket volume	5	3.5%
Neutron power absorbed	17	12 MW
Fraction of total neutron power	1	.7 %
RF power coupled per antenna	0.5	0.75 MW
RF coupled power density	1.5	2.25 MW/m^2
RF peak voltage at 2 ohms	20	25 kV

4. DEVELOPMENT OF LOWER HYBRID LAUNCHERS

4.1 Background

Lower hybrid heating and current drive depend on the excitation of the so-called slow wave which propagates nearly parallel to the magnetic field with the electric field vector aligned with the magnetic field. The frequency is typically in the range 1-10 GHz. The wavelength parallel to the magnetic field is less than the vacuum wavelength and defined by the so-called $N_{//}$, which is the ratio of the vacuum wavelength to the parallel wavelength in the plasma. This parameter determines the angle of propagation of the wave relative to the magnetic field and thus the trajectory within the plasma. It also determines the damping mechanism.

For ion heating, the preferred $N_{//}$ is typically above 10. The corresponding wave progagates at a substantial angle to the field, penetrates well into the bulk of the plasma, and is damped by the ions. However, for current drive applications, much lower values of $N_{//}$ are required, typically around 2. These waves propagate nearly parallel to the magnetic field and may only penetrate into the outer part of the plasma, and are damped by the electrons. This damping occurs preferentially on those electrons travelling near the phase velocity of the wave and thus results in a nett current.

The role of the lower hybrid launcher is to excite this slow wave. This requires the generation of an RF electric field polarised parallel to the magnetic field with a spatial distribution along the field matching the wavelength of the desired wave, and at a minimum density determined by the cut-off frequency. This cannot be simply achieved by irradiation by vacuum electromagnetic waves as it requires a spatial disribution of the electric field on a scale which is small compared to the vacuum wavelength. Various proposals have been made to overcome this problem. These include the use of a waveguide array mounted close to the edge of the plasma [LALLIA, 1974; BRAMBILLA, 1976], the use of an array of rods close to the plasma [PETELIN et al, 1989], diffraction from which also produces the required field distribution, and beating of two or more waves of higher frequency and thus shorter wavelength [COHEN, 1983].

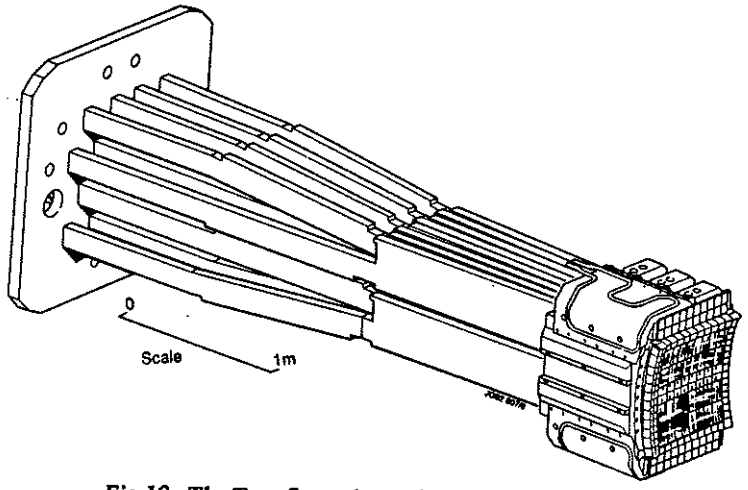

Fig 10. The Tore Supra lower hybrid launcher

All presently operating systems utilise the waveguide array, as illustrated by the Tore Supra launcher in Fig 10. A rectangular waveguide will propagate if the waveguide height is greater than about one half of the vacuum wavelength. Single mode will be obtained if the height is less than one wavelength and the width less than one half wavelength. The waveguide will continue to propagate on this mode as the width is reduced to a value much less than the wavelength. By arranging an array of narrow waveguides, it is therefore possible to produce an electric field distribution which is polarised in the narrow direction of the waveguide and has a spatial variation on the scale of the waveguide width which can be small compared to the vacuum wavelength. Introducing a controlled phase shift between waveguides results in a field distribution which propagates across the array with a velocity and thus $N_{//}$ which is determined by the phase shift. In vacuum, such an array will not generate a propagating electromagnetic wave if the $N_{//}$ is greater than 1; all the power will be reflected from the grill. However, if this array is now mounted radially with the grill mouth projecting into the edge plasma such that the density at the grill mouth is above cut-off(typicaly $10^{18}/m^3$), this array will couple to the corresponding lower hybrid wave in the plasma.

The array of rods has been investigated theoretically, but as yet has not been tested on a plasma. This system has some major advantages compared to the waveguide array and will be discussed further below.

The beating of waves has been assessed analytically. The coupling to lower hybrid waves is a second order process and the predicted coupling efficiencies are too low to be of interest. Such a scheme has the major advantage of having no coupling structure close to the plasma, as is essential to all other methods. This may justify further theoretical studies of such schemes. However, whilst the main impediment to the application of lower hybrid current drive to next generation machines remains the overall efficiency rather than the coupling structure, the main thrust will continue to be in better understanding of the physical processes in the plasma.

4.2 Design of present systems

Multi-megawatt launchers are in operation on various tokamaks, including JT-60U [SEKI et al, 1990], Tore Supra [REY et al, 1988] and JET [KAYE et al, 1988]. The main design parameters of these systems are summarised in Table 5. The

system on JT-60 had the potential for coupling about half of the installed power to the plasma, and indeed achieved a maximum of 9 MW. A new series of launchers is being developed for JT-60U, the first of which is presently operating.

The system at Tore Supra is now fully installed and operational. This system uses two launchers with the ultimate potential to couple about 6 MW to the plasma. The JET prototype system has been operational for two years with the potential to couple around 3.5 MW, and the full system is being installed in the present shutdown. All of these systems have an $N_{//}$ of about 1.8, and are designed for current drive applications.

Table 5. Design and performance parameters of some lower hybrid systems. Figures in brackets indicate imminent upgrades.

	Installed Power MW	Coupled Power MW	Coupled Energy MJ	Frequency GHz	No Launchers	Waveguides/ Launcher	No Windows/ Launcher
JT-60	24	9	20	1.7/2.2	3	-	-
JT-60 U	3(10)	1.8	-	1.7/2.2	1(3)	96 (192)	16
Tore Supra	8	6	150	3.7	2	128	16
JET	5(15)	2.4	50	3.7	1	128 (384)	16(48)

A typical system comprises a power source, transmission lines, splitting network, vacuum windows and a waveguide array close to the plasma. Klystron amplifiers are used as primary RF sources with output powers up to 1 MW per klystron at 2 GHZ, 0.6 MW at 3.7 GHz, 0.4 MW at 8 GHz. A single oscillator is used to drive all klystrons in parallel,with active phase shifters on the low power side for controlling the phase. Either standard single mode waveguides or oversize single mode guides route the power to the torus, with typically one guide per klystron. Some systems (JET, ASDEX) use circulators to protect the klystrons from reflected power. This can simplify the launcher design, which must otherwise be designed to have very low reflected power.

In designing the launcher, previous generation projects and the smaller present generation projects, for example FTU [ANDREANI et al, 1990] and PBX [GREENOUGH et al, 1991] favoured locating the window close to the plasma in order to minimise the multipactor arcing problem. The splitting network is then external to the vacuum system, and typically utilises hybrid junctions for the purpose. This approach is not feasible on reactor systems, due to neutron irradiation of the windows, and JT-60U, Tore Supra and JET have all found it preferable to locate the windows remote from the plasma and use internal multijunction splitting networks.

4.3 Splitting Networks

The output power from a single klystron is much greater than can be coupled on a single waveguide at the grill mouth. Typically, each klystron drives 8-16 wavegides at the grill. Substantial splitting networks are therefore required. Whilst the amplitude and phase of the klystron is variable, this clearly only allows parallel adjustment of many waveguides. Thus the splitting network will partly determine both the amplitude and phase distribution, and thus $N_{//}$, at the grill mouth. The network may also be sensitive to reflected power from the grill. Both the amplitude and phase of this reflected power are dependent on the plasma load and thus ill-defined. The splitting network design will determine the sensitivity to reflected power.

Hybrid junctions or magic T's are widely used to divide the incoming power to suit the launcher. Such 4-port junctions may have a matched load on the fourth port. This has two substantial advantages. Firstly, the power split and phase distribution is independent of the reflected power from the launcher. Secondly, the junction can be designed to partly fulfill the role of a circulator by deflecting much of the reflected power into the matched load.

Some smaller systems (ASDEX, PBX, FTU) use external 4-port junctions with matched loads to complete all power splitting, the output from the splitting network mapping one-to-one onto the grill mouth waveguides. Such systems decouple the forward and reflected power, the amplitude and phase at the grill being totally defined by the network and independent of the reflection. These systems may also have variable phase shifters in each output line which enable continuous adjustment of the $N_{//}$ spectrum. In the case of PBX, this adjustment uses active (ferrite) components which enables on-line adjustment. This system operates on a short (1 second) pulse length and the presently used phase shifters are not rated for the continuous duty required of next step machines.

Splitting networks such as these are in principle ideal in giving total definition and control of the spectrum. Furthermore, in present devices with low neutron loads, it enables the windows to be located close to the plasma and thus avoid multipactor arcing at the electron cyclotron resonance layer (to be discussed below). However, for next step devices, the resulting system has important disadvantages. The system is expensive and cumbersome. It is necessary to provide individual windows for each waveguide at the grill, possibly many thousand; these windows must be screened from neutrons and thus remote from the plasma. The reflected power is wasted, in turn requiring provision of more klystrons and associated expense.

An alternative which overcomes the window problem is to install some or all of the junctions inside the vacuum system. This is widely done on current devices (JET, Tore Supra, JT-60U). External splitting is used only to the extent necessary to achieve acceptable reliability of the vacuum windows. Typically, such windows are based on the klystron windows, and thus can handle similar power. Thus, external splitting by a factor two using 4-port devices is common. By choosing the lengths of the two lines from the junction to the grill appropriately, reflected power from the launcher may be diverted to the load. The junction then acts as a circulator in reducing the reflected power to the klystron.

Internal splitting may again use 4-port junctions. The systems on JET and Tore Supra both achieve one factor 2 split with hybrid junctions, in the former case with a matched load to decouple forward and reflected power, and in the latter case, with short circuit termination of the fourth port. The prototype launcher on JET includes modules of both JET and Tore Supra design. A comparison of the two systems has been carried out in some detail with regard to reflected power, losses and current drive efficiency. The results of this study are inconclusive due to other differences in the 2 modules, but suggest better control of the spectrum and lower standing wave ratio in the grill on the JET module consistent with expectation [DOBBING et al, 1992].

A powerful technique which combines the function of the splitting network, phase shifters and circulators has been developed at Petula [NGUYEN et al, 1982; GORMEZANO et al, 1985]. This is the so-called multijunction. A typical multijunction is illustrated in Fig 11. The incoming waveguide is split using two successive (3-port) E-plane junctions into 4 waveguides at the grill. After each junction, phase shifters are incorporated into each line as illustrated. These have the effect of producing, in this example, a 0-90-180-270 degree forward power phase distribution at the grill. Consider also the phase distribution of the reflected power at the second junction. The reflected power in the 2 guides at this junction is now 180 degrees out of phase. These cancel and the reflected power is in turn reflected from the junction back to the grill. On the second reflection, the phases are such as to add and the wave propagates back towards the klystron. The overall reflection co-efficient measured at the input is now squared and the reflected power to the klystron much reduced.

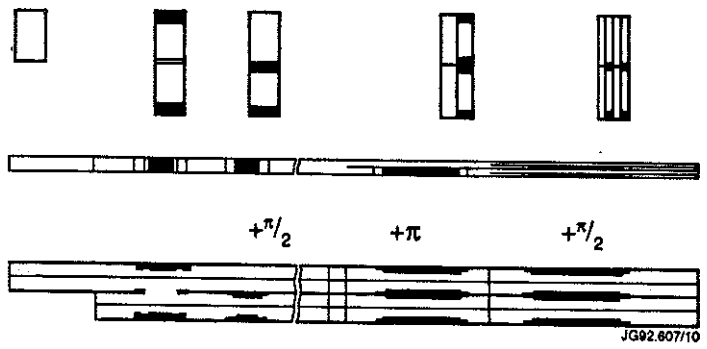

Fig 11. A typical multijunction

A detailed numerical model of the multijunction has been developed, the so-called SWAN code [MOREAU et al, 1983]. This confirms the low overall reflection co-efficient and also the good directivity of the amplitude and phase distribution at the grill mouth. The multijunction thus gives a very compact system giving low reflected power.

There are many variations on this design based on the same principle. For example, Tore Supra and JET use an E-plane junction dividing the output into two with 90 degree phase difference. JT-60 used a junction from one to 3 output waveguides with a 60 degree shift between guides.

JT-60U, JET and Tore Supra now all use multijunction grills which operate well and give current drive efficiencies similar to conventional grills.

It should however be noted that multijunctions have disadvantages. The use of three port junctions means that the forward and reflected power are not decoupled. Thus, both the amplitude and the phase distribution at the grill mouth are dependent on the amplitude and phase of the reflected power. Precisely in the operating regime of high reflected power where the multijunction offers the most benefit, the amplitude and phase distribution at the grill are not fully defined by the input amplitude and phase, and are not readily deduced from external measurements of the reflected wave. Typical results computed using the SWAN code for the JET prototype launcher are shown in Fig 12. It is seen that the directivity falls from 65 to 50% with a refection co-efficient of 6% (corresponding to 25% at the grill). Furthermore, this loss in directivity is associated with a non-uniform power distribution across the grill. Thus, the computed peaking factor on the electric field in the grill is seen from Fig 12 to be a factor 2 at 6% reflection. This may be compared to a factor 1.7 in a conventional grill at 25% reflection for the same coupled power. This corresponds to a factor 1.4 in mean power density at the same peak electric field.

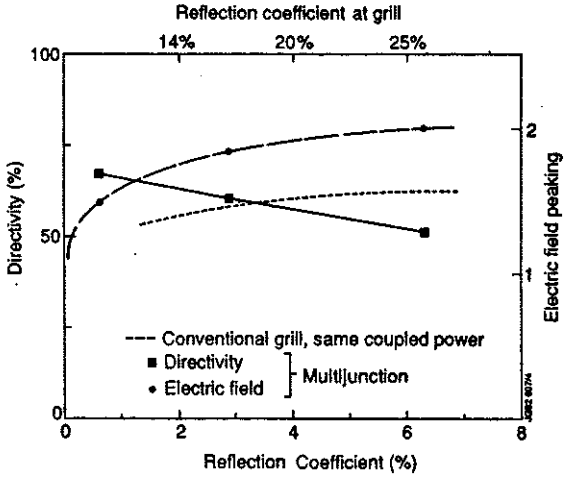

Fig 12. Effect of reflection on the directivity and on the peak electric field in the most heavily loaded waveguide of the JET prototype grill, computed using the SWAN code. Also shown is the electric field in a non-multijunction waveguide coupling the average power of one guide in the grill.

This effect depends on the length from the grill to the first E-plane junction. The results of a numerical simulation of the JET grill using the SWAN code have been used to minimise the sensitivity to the phase of the reflected power on the JET launcher [MOREAU et al, 1987]. The data of Fig 12 are for this optimised grill.

A histogram of the operating power of one of the klystrons on the JET prototype launcher is shown in Fig 13, together with the corresponding power density averaged over the grill mouth. A slow improvement with time is clear as the launcher conditions. The maximum power density achieved at the end of the campaign is 50 MW/m^2. However, the value which could be routinely achieved has only increased to typically 35MW/m^2 by the end of the campaign.

The limiting performance of the present generation of multijunction grills is summarised in Fig 14. After extended conditioning, the indicated range of coupled power densities in the waveguides at the grill mouth can be achieved on Tore Supra and JET. The points given for JT-60U are the design points, which are based on the extensive experience with high power launchers on JT-60. Also shown in Fig 14 are previous results from many experiments as summarised by [TONON, 1989].

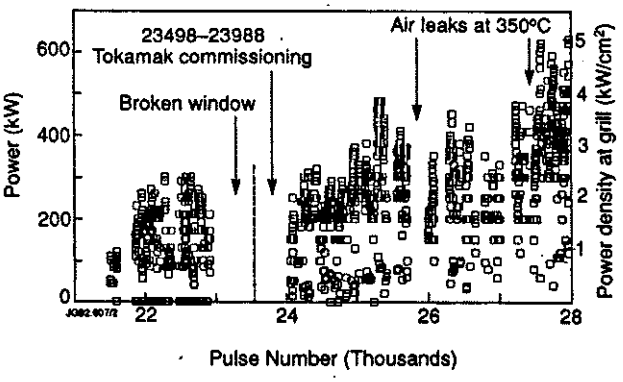

Fig 13. A histogram of the operating power of one of the klystrons on the JET prototype launcher.

It is clear that even the best present data falls significantly below the previous trend line. This may be a consequence of the multijunction. The factor 1.4 reduction in mean power density at given peak field when the reflection is above 20% at the grill (4% from the launcher) would largely account for the difference. The most heavily loaded waveguides may indeed be operating near the trend line? This data suggests a design value at 5GHz for routine operation of multijunction arrays of 35 MW/m^2 averaged over the area of the grill.

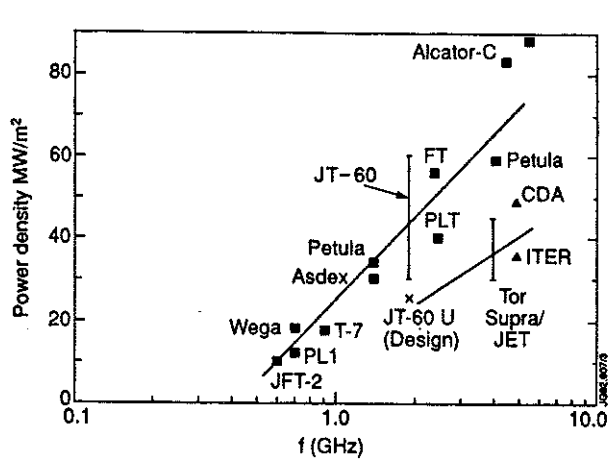

Fig 14. The maximum and typical power density at the grill of present launchers. The results for previous generation systems and the trend line derived from that data are shown for comparison.

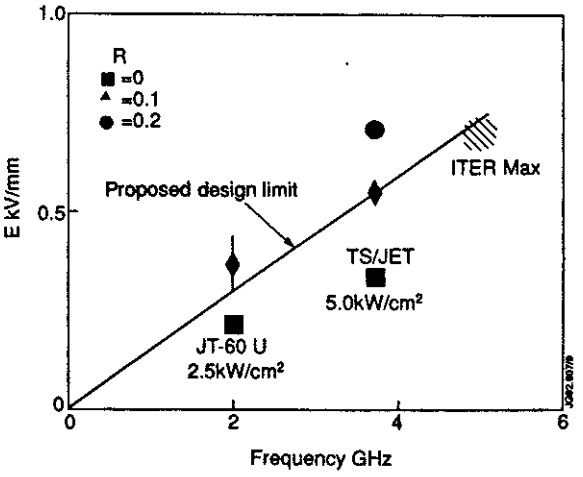

Fig 15. Peak electric field in the waveguides of present systems and suggested design limit for next step machines.

The maximum electric field in the waveguide may be more significant than the power density, as this is strongly dependent on reflection co-efficient. These data are given in Fig 15 for various reflection co-efficients. The data for JT-60U is again the design value for the new launcher. The JET/Tore Supra data is for 50 MW/m^2, using the peaking data in Fig 12. A linear trend as expected from multipactor scaling is consistent both data points and suggests a peak field at 5 GHz of 0.8 kV/mm. This corresponds to a design field of 0.7 kV/mm at the design power density of 35 MW/m^2 suggested above.

The contour corresponding to 0.7 kV/mm is shown in Fig 16, together with the operating power of one of the JET klystrons plotted against reflection co-efficient from the launcher. It is observed that the maximum klystron power varies with reflection co-efficient as expected if the electric field is the limiting parammeter, up to a reflection co-efficient of 15% (40% at the grill mouth). At sufficiently low density, a higher field can apparently be sustained.

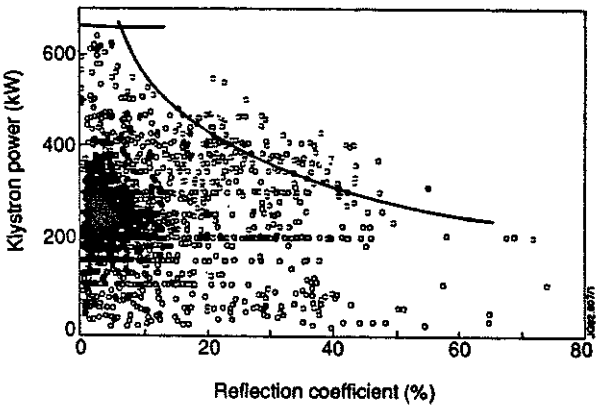

Fig 16. Output power of one of the JET klystrons for all pulses since start of operations plotted against reflection co-efficient from the launcher. Also shown are the maximum klystron power and a contour of constant electric field in the waveguide at the grill month.

4.4 Vacuum Windows

The vacuum window is a critical part of any LH system. Present systems fall into one of two categories. Some systems locate the windows as close as possible, typically 0.5m, to the grill mouth. This has the important advantage of placing the electron cyclotron resonance zone outside the vacuum system and thus avoiding the multipactor arcing at this zone. Such systems are found to condition easily. However, this approach is not applicable where active cooling or remote handling of the windows is required, or in next step devices where the neutron fluence close to the plasma prohibits the location of ceramics in this region.

The second category, including JT-60U, Tore Supra and JET, locate the window far from the plasma, with internal splitting networks. This approach minimises the number of windows, which is determined by the power handling capability of an individual window. It also enables the window to be screened from the high neutron fluence and to be handled remotely. The disadvantage of this approach is that the electron cyclotron resonance is likely to be inside the vacuum system, as on JT-60U, Tore Supra and JET. The resulting multipactor arcing causes severe problems with conditioning of the launcher.

It may be possible to overcome this problem in next step machines by locating the windows inside the cyclotron resonance with additional massive neutron screening for the windows. This has been proposed for ITER [TONON, 1990].

High power windows are similar to klystron windows. Long pulse or steady state operation at hundreds of kilowatts is routinely achieved using water cooled, beryllium oxide, pill-box ceramics. The JET window has two such ceramics in series with a pumped and monitored interspace to ensure integrity of the tritium confinement. The ratings of presently used windows are summarised in Table 6. The power scales inversely with the frequency as expected for edge cooled windows. Extrapolating to 5 GHz gives a power of 200 MW per window for the same margins of safety and with no allowance for degradation under neutron irradiation.

Table 6. Design ratings of lower hybrid windows and extrapolation to next step machines.

	Frequency GHz	Power/Windows kW	No Windows
JT-60	2	450	16
Tore Supra	3.7	250	32
JET	3.7	300	48
ITER CDA	5	200	250

4.5 Multipactor arcing

Multipactor arcs have been recognised as a problem with RF sytems in vacuum for many years, in space and particle accelerator applications as well as fusion reearch. The mechanisms involved are well understood. An electron at a surface is accelerated by the RF field. On impact with a surface, this electron releases secondary electrons. If this impact co-incides with a reversal of the RF field, these secondary electrons are accelerated back to impact the first surface. This can result in an avalanche process if the secondary electron emission co-effient (SEC) is greater than one.

The condition for breakdown is that the electron transit time must equal the RF half period, or its harmonics. The problem can arise with two surface multipactoring, where the condition for breakdown is that the electron transit time equals the RF half period or its harmonics. In addition, in the presence of a magnetic field, single surface multipactoring can occur, where the condition for resonance is that the electron gyrofrequency equals the RF frequency or its sub-harmonics. The first subharmonic is usually the most severe. Single surface multipactoring cause severe problems with LH systems and has been studied in detail at JT-60 where good correlation is found between experiment and theory [SAKAMOTO et al, 1986].

Control of multipactoring has been achieved by various means with varying success. All methods depend on producing a SEC at the surface which is less than unity, even at grazing angles of attack in the case of single surface arcing. Techniques used include:

- Glow discharge cleaning of the surface
- RF discharge cleaning (conditioning)
- Baking combined with RF discharge cleaning
- Coating of the surface with low SEC material, eg carbon
- Coating of the surface to produce a rough finish on a micron scale length
- Selection of surface material (copper, silver, gold)

The discharge cleaning methods have been used on stainless steel, titanium and copper. An electrode is inserted into the waveguide mouth and a low pressure glow discharge struck between the electrode and the grill. This may be done before installation. It is found that the beneficial effects are partly retained after subsequent exposure to air. Electrodes have also been incorporated into the launcher grill and used to condition the grill in situ. Such a technique is not practical on large arrays with close-packed waveguides.

RF conditioning, using repetitive short, high power RF pulses in vacuum, is widely used and effective but very slow and time consuming. Many thousands of pulse are required. Furthermore, the standing wave ratio is very high without plasma and the conditioning is apparently not fully effective over the complete surface. It is found to be also necessary to condition with plasma. The effectiveness of this process is strongly dependent on temperature. A regime of conditioning at elevated temperature followed by operation at a temperature typically 50 C lower has been found to give much improved results at JET. As the temperature increases during operation, so the power handling capability falls again. Outgassing of the surface is thought to be the key process.

Coating of the suface with various low SEC coatings is also effective. Materials explored for tokamak applications include carbon, amorphous CH structures,TiC, boron carbide. Of these, none except the (CH)n structures have been found to have a SEC below unity at grazing incidence. The (CH)n coating is unstable above 300 C, but may be useful on cooled waveguides. Tests have shown suppression of multipactors on copper by coating with carbon [KAYE et al, 1988], and carbon has been used in JT-60 and JET. In the latter case, lack of adhesion led to failure of the coating. Heavy outgassing is also a difficulty with carbon.

Producing a surface which has high roughness on a 1-10 micron scale length has been shown to be very effective in suppressing multipactor arcs, even when the material itself has a SEC above unity. This is due to the capture of the secondary electrons in the rough surface. In particular, the so-called black gold [DERFLER, 1984] surface treatment has been successfully used on ASDEX. The grill with this surface treatment required a minimum of conditioning and coupled high powers to the plasma.

There are two disadvantages to this procedure. Firstly, the rough suface is inherently much more resistive than the solid material, and must be typically 10 micron thick to be effective. Such a surface is inherently lossy unless semi-conductor materials (such as boron carbide) are used such that the skin depth is large compared to the thickness. Thus, black gold was found to have losses 4-7 times higher than copper at 3.7 GHz. This is not acceptable in next step devices. The second problem is that the rough structure has a large surface area and can result in heavy outgassing during long pulse operation. Amorphous carbon layers, which have very low losses, suffer severely from this problem.

Selection of materials can alleviate the multipactor problem. The peak power capability of a waveguide coated with dense silver was found to be substantially higher than an identical guide coated in copper [KAYE et al, 1988], and without the appearance of multipactor arcs. This is consistent with similar observations during conditioning of ion cyclotron systems [KAYE et al, 1987]. Recently, gold has been found to give better results on the latter [WEDLER et al, 1992]. Gold avoids the induced activity problem of silver under neutron irradiation.

A combination of precious metal coating with high temperature baking during conditioning shows the most promise for suppressing multipactors in the electron cyclotron resonance zone in reactor scale systems.

4.6 Grill Fabrication

Various methods have been used to fabricate the grill structure. Structures not using the multijuntion principle are in general simpler to fabricate as they have neither the junctions nor, in particular, the phase shifters. These grills commonly use extruded waveguide section in close packed arrays or machine the grill from solid. In the case of FTU, the copper coating is co-extruded with the waveguide. JET use extruded stainless steel waveguide for the vacuum connection from the window to the multijunctions. This is an effective and economical process.

Multijunctions have been fabricated by vacuum brazing pre-machined parts in a single operation (Tore Supra, JT-60), and by machining of 2 x 3 m long half multijunctions and vacuum brazing of the longitudinal joints (JET).

Of the presently operating systems, only that at Tore Supra is actively cooled. This system uses longitudinal channels in extruded copper/zirconium alloy to carry high pressure water at 150 C. In next step devices, such cooling will be essential, and with it the use of materials of good thermal conductivity. The associated high electrical conductivity of metals compounds the problem of disruption forces on the system. Waveguides have been produced in carbon fibre material with copper lining which avoids this problem and has interesting potential for this application. The newly developed dispersion-hardened 'Glydcop' material is also being considered, and the launcher for Tokamak de Varennes is being fabricated in this material [DEMERS et al, 1992].

4.7 Side protection

The sides of the grill are normally protected from the plasma by tiles of refractory material, often graphite. The grill is normally contoured to lie on a magnetic surface. The tiles are postioned to be in front of the magnetic surface containing the grill. The radial separation is a critical parameter in determining the reflection from the grill mouth. The connection length across the grill is small (typically 0.2-0.5 m) and the scrape-off layer between the tiles typically sub-millimetre. Thus each millimetre clearance can represent an order of magnitude in density at the grill. Experience on ASDEX [LEUTERER, 1991] has shown the strong sensitivity to this clearance. The optimisation of the position of the side protection is thus a difficult trade-off between protection from the plasma and loss of coupling.

4.8 Launcher Position Control

The reflection from the grill mouth is sensitive to the density at the grill. The position of the grill relative to the torus wall has been adjustable off-line in many devices. Recently, the launchers on JET and Tore Supra have been equipped with the facility for rapid on-line position control. These systems use hydraulic cylinders controlled by electro-hydraulic servo valves in closed-loop configuration to set the position. The JET system achieves sub-millimetre positional resolution with typically 150 ms response time to small changes [WALKER et al, 1992]. This system has been used to control the launcher position for volt-second saving during ramp-up of 7 MA pulses, as shown in Fig 17, and also in closed-loop control of the reflection co-efficient.

JT-60 [IKEDA et al, 1990], ASDEX [LEUTERER et al, 1991] and Tore Supra [LITAUDON et al, 1992] find that the coupling can be much less sensitive to position of the grill than anticipated, due to unexpectedly high density at large distances from the last closed flux surface (LCFS). At ASDEX, it has been observed that the good coupling at large distances is dependent on first establishing good coupling close to the plasma, and that the coupling can suddenly fall to expected values as the launcher is withdrawn. It is thought that this effect may be due to the creation of a private plasma by the LHCD itself. JET conversely find that the coupling correlates well with scrape-off layer connection length as shown in Fig 18 [EKEDAHL, 1992]. The launcher coupling is much less sensitive to position when the launcher is in front of the ICRF antennae, but only to the degree expected from the increase in scrape-off layer thickness. (The coupling of the antennae was however reduced and there may be a conflict of interest between the two systems in this regard). It is not clear that a private plasma can be sustained at extended distances from the LCFS in next step machines or that good current drive efficiency can be maintained in these conditions.

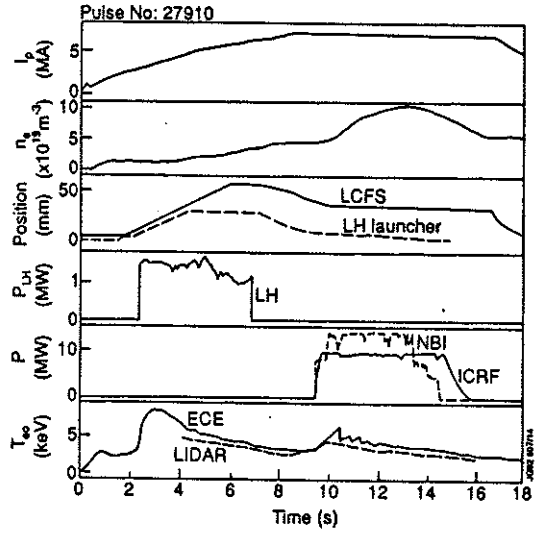

Fig 17. Results of a 7MA pulse on JET in which the launcher was moved inwards in front of the limiters during the current ramp and then withdrawn for protection during the flat top.

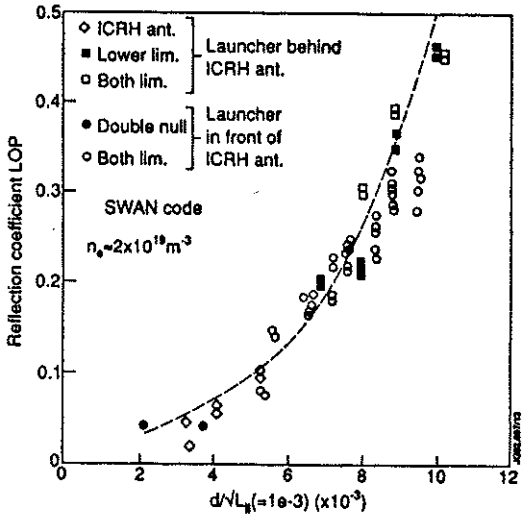

Fig 18. Correlation of JET coupling data with scrape-off layer connection length and the SWAN code.

5. LHCD LAUNCHER REQUIREMENTS ON NEXT STEP DEVICES

Next step machines will impose important new requirements on the design of LHCD launchers. Accessibility and current drive efficiency considerations at high density lead to an increase in frequency, a value of 5 GHz being adopted for the ITER design study. This reduces the waveguide dimensions and increases the number of waveguides for a given power linearly with frequency, taking account of the higher power density at the grill.

As discussed above, the experimental data from present machines suggests that the power density that can be routinely achieved is barely half of the previous trend line. If the designs of Tore Supra/JET and of JT-60U are extrapolated to higher frequency assuming the same $N_{//}$ and the same phase shift between adjacent guides, the number of waveguides required to couple the 50 MW of power proposed in the ITER CDA [PARAIL, 1991] is as given in Table 7. A total of 3-4500 guides would be required, depending on frequency. This may of course be reduced somewhat by increasing the phase shift and thus the waveguide width without degrading the spectrum on such a large array. Nonetheless, it is clear that any such launcher will be a formidable device, the more so as the frequency increases. The tolerance to which the guides must be manufactured also scales inversely with frequency and will be typically +/-0.1 mm at 5 GHz.

Table 7. The total number of waveguides obtained by extrapolation of present multijunction designs to a 50MW system for the next step.

	Frequency GHz	Power Density, MW/m^2	No Waveguides 5GHz	8GHz
TS/JET	317	35	2800	4000
JT-60 U	2	25	3300	4500

The number of windows required based on present technology is given from the data in Table 6 as 250. This makes no allowance for neutron degradation. Any such degradation will require an increase in the number of windows or a narrowing of the safety margins. Thus, accepting an increase from $1x10^{-4}$ to $2x10^{-4}$ in loss tangent doubles the number of windows! There is little data on the effects of neutrons on the loss tangent of beryllia. JET have had samples tested up to 10^8 rad with

a degradation which could not be resolved within the accuracy of the measurements. Irradiation data is urgently required for beryllia and such tests are in progress.

Results on alumina suggest that the neutron fluence will need to be less than $10^{22}/m^2$ [PARAIL et al, 1991]. This would imply heavy screening, the effectiveness of which needs careful analysis taking account of scattering, or location of the windows outside the cryostat, and thus ouside of the electron cyclotron resonance. The splitting network will be largely inside the torus vacuum and will likely use the multijunction technique. The system must operate long pulse (at least 1000 seconds) and is effectively in steady state. Cooling of the grill will be essential, both due to RF heating and neutron irradiation. Total weight has been estimated at 120 tonne for each of two launchers. The position of the grill needs to be adjustable, but only slowly due to the near steady state operation. The position of the grill mouth must be behind the first wall for protection from alpha particles and runaway electrons, but nonetheless sufficiently close to couple power efficiently. Erosion of the grill due to the heat pulse during disruptions and normal plasma operation needs to be analysed, and the material of the grill chosen accordingly.

This amounts to a very demanding engineering design and manufacturing problem. The attractiveness of LHCD would be much enhanced by the development of substantially simplified in-torus systems for next generation devices.

6. INNOVATIVE LHCD DEVELOPMENTS

There have been a number of proposals for simplifying the conventionasl launcher or for alternative coupling structures which may offer major advantages in next step machines.

Consider first the possibility of simplifying the existing systems. The essential requirement is the array of waveguides with the correct phase distribution at the grill mouth. In addition, window technology and the properies of materials effectively define the vacuum boundary. The coupling between these two boundaries may be achieved other than by using the present discrete waveguides.

6.1 Oversized waveguide

The new launcher being developed for JT-60U [IKEDA et al, 1991] will utilise a single oversize waveguide to drive each block of 12 output guides, as illustrated in Fig 19. A test assembly of this system has been constructed and tested with favourable results. For example, the higher order mode content is less than 10% and the predicted current drive efficiency based on a weighted $N_{//}$ spectrum degraded less than 10%. The JT-60 klystrons have a frequency scanning capability which can be used to control the $N_{//}$ produced by this grill over the range 1.4-2.4. A simple method of fabrication is also proposed using vacuum brazing. It may be that this approach can be extended to a larger number of waveguides.

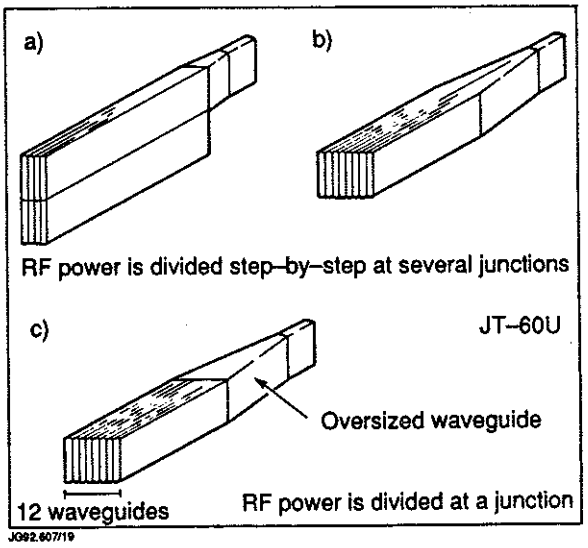

Fig 19. The use of oversize waveguide on the new JT-60U launcher.

6.2 Hyperguide

JET have taken this approach further and propose also to use the overmoded guide at the input. This so-called hyperguide would operate on a single high order mode. It would be driven by many incoming single mode guides and would couple to many outgoing single mode guides. JET consider to replace all 48 waveguides with a single TE 0,12 guide, as illustrated in Fig 20. Numerical analysis of the mode stability of TE 0,12 waveguides suggests that it is possibleto efficiently propagate in this mode using excitation by discrete incoming waveguides (48 in total in a 6X8 array) and termination by a short waveguide array of 384 guides. Each element of the incoming array is arranged to have the same phase and amplitude (by control of the asociated klystron). The output array is excited also with equal amplitudes but with 180 degree phase shift between rows. The required phase at the grill mouth is established by phase shifters within the output waveguide array, which may also contain E-plane junctions . These complicate and increase the length of the array but reduce reflection back into the oversized guide and may be essential for this purpose.

This general system is being analysed using JET parameters. Initial results are encouraging in that it appears to be possible to suppress unwanted modes. Suitably slotting the walls of the oversize guide may further improve the mode selectivity.

Such a waveguide would enable the replacement of many guides by just one guide, in particular in the critical electron cyclotron resonance region. This much simplifies the manufacture, reduces the surface area, RF losses and the outgassing by a large factor, and alleviates the multipactor problem due to the reduced area and the much enhanced vacuum conductance available in the guide.

At present, this proposal is only in the conceptual design phase.

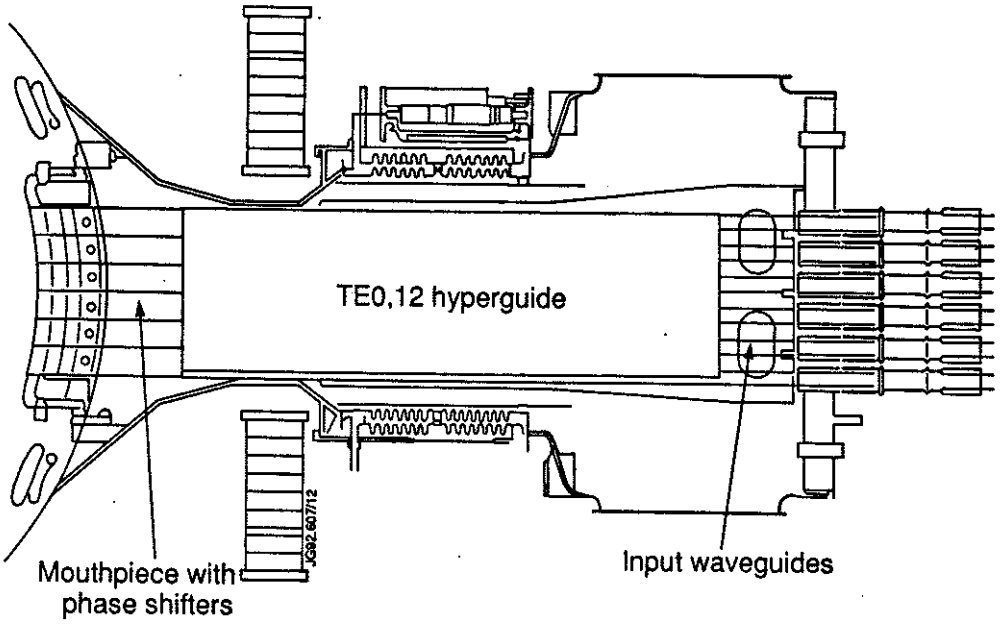

Fig 20. The hyperguide as it would be applied to the JET launcher.

6.3 Quasi-optical System

A fundamentally different alternative to the waveguide array has been proposed by [PETELIN et al, 1989]. In its simplest form, it comprises a single row of parallel rods mounted in the edge plasma. These rods are spaced at regular intervals and irradiated at an angle such that the only propagating diffraction lobe from the array excites the required $N_{//}$ slow wave. This is ilustrated in Fig 21.

Such a system offers major advantages over the waveguide array. In particular, the plasma facing array is of simple and robust construction. Considerable theoretical analysis of such a system has been carried out [PETELIN et al,1989; KOVALYOV et al, 1990] and has identified a number of difficulties. In particular, the reflection from a single row is high, perhaps 90%. The proposed solution to this problem is to provide a second array of rods, such that the reflections from each row cancel. This solves the immediate problem of loss of power, but inevitably results in a high standing wave ratio between the two rows. The electric fields in this region will be a factor 5-10 higher than in a waveguide array at the same coupled power density. This may well limit the coupled power density to a level much less than in conventional grills.

The requirement to irradiate the array at an angle also complicates the structure in reactor scale devices, necesitating the provision of suitable high power reflectors in the port. The optical train is likely to be similar to proposals for ECRH application to next step devices, with the complication that the factor 20 increase in wavelength at lower hybrid frequencies will enhance diffraction effects in the optical train and reduce both the power and uniformity of illumination of the array.

This proposal also has not been tested in a Tokamak environment. A detail design of a system for FTU is being developed.

The credibility of this technique depends critically on its successfull demonstration in such an experiment. However, the potential advantages in design of high power lower hybrid systems for reactor scale devices makes such a demonstration a high priority.

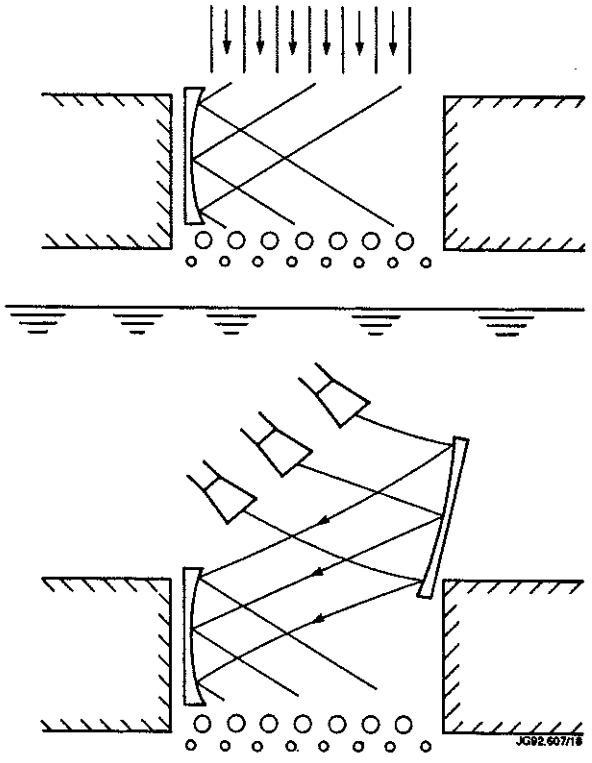

Fig 21. The rod-array coupling structure.

7. CONCLUSIONS

The design features of the major ICRF antennae have been reviewed and some limits to performance identified. Improvements in understanding of impurity production mechanisms have led to important advances in performance of existing systems over the last several years. Recent developments in the use of boron carbide as a cladding material, or even operation without screens, may lead to further advances. Simple antenna modifications can enhance the coupled spectrum for fast wave current drive applications. The folded waveguide antenna has interesting potential for very high power density operation should this be required.

The technical requirements of antennae for next step machines has been considered. Many antennae mounted in the blanket above or alongside the ports can meet the anticipated requirements for heating and FWCD with power density, power per antenna and line voltage comfortably within the operating range of existing systems.

Lower hybrid systems are currently in operation on various large Tokamaks around the world. Coupled power levels up to 9 MW have been achieved. These devices all use waveguide arrays and the design of these has been reviewed. Many difficult technical problems have been overcome in the provision of these launchers, which remain complex and delicate systems.

The requirements of lower hybrid systems on next step devices raise further constraints on the design, largely due to neutron irradiation, steady state operation and increased frequency, together with the 100 MW scale of such a facility. Whilst existing technology could be used to construct a launcher, it would be a highly complex device.

The attractiveness of LHCD on next step machines would be much enhanced by the development of simpler coupling structures. Such structures have been proposed but require demonstration at high power on operating tokamaks to establish their viability.

ACKNOWLEDGEMENT

The author acknowledges many constructive remarks from J Jacquinot, C Gormezano, T Wade and many others in RF division at JET, and provision of klystron statistics by P Schild.

REFERENCES

ANDREANI, R. et al (1990). Fusion Technology, London, 1084
ARBEZ, J. et al (1984). Heating in Toroidal Plasmas, Rome, 1244
BAITY, F.W. et al. Contr. Fus. and Plasma Heating, Schliersee, 2, 157
BAITY, F.W.et al (1991). Radio Frequency Power in Plasmas, Charleston, 298
BEESTON, J.M. et al (1984). J. Nuclear Materials, 122, 802
BEAUMONT, B.et al (1992). Boulder Workshop
BEHRISCH, R. et al (1987). Contr. Fus. and Plasma Phys., Madrid, 778
BHATNAGAR, V.P. et al (1990). Proc Joint Varenna Lausanne Int. Workshop: Theory of Fusion Plasmas, Varenna, p.243
BHATNAGAR, V.P, JACQUINOT, J.et al (1991). Radio Frequency Power in Plasmas, Charleston, 115
BHATNAGAR, V.P.et al (1991). IAEA Tech.Comm. Meeting on FWCD in Reactor Scale Tokamaks, Arles, 110
BRAMBILLA, M. (1976). Nucl. Fus., 16, 1, 47
BROWN, T. (1992). Design Study of the NET ICW Antennae, Final Report
BURES, M. et al (1991). Plasma Phys. and Contr.Fus., 33, 8, 937
BUTTERWORTH, G.J. (1988). Fusion Technology, Utrecht, 231
CARTER, M.D.et al (1991). Radio Frequency Power in Plasmas, Charleston, 164
CATTANEI, G.,MURPHY,A.B. (1989). Nucl. Fus., 29, 1, 15
CHODURA, R. and NEUHAUSER,J. (1989). Contr. Fus. and Plasma Phys., Venice, 1089
COHEN, B. (1983). LLNL Report UCRL-89871
DEMERS, Y. et al (1992). This conference.
DERFLER, H. et al (1984). Heating in Toroidal Plasmas, Rome, 1261
D'IPPOLITO, D.A. et al (1990). Fusion Eng. and Design, 12, 209
D'IPPOLITO, D.A. et al (1991). Plasma Phys. and Contr. Fus., 33, 8, 937
DOBBING, J. et al (1992). Fusion Technology, Rome (to be published)
EKEDAHL, A. et al (1992). This conference.
EQUIPE TFR (1978). Nucl. Fus., 19, 11, 1538
FUJII, T. et al. (1990). Fusion Technology, London, 1171
FUJII, T. et al (1991). Fusion Engineering, San Diego, 107
GORMEZANO, C. et al (1985). Nucl. Fus., 25, 419
GORMEZANO, C. (1991). Fus. Eng. and Design, 14, 99-109
GORMEZANO, C. et al (1991). Fast Wave Current Drive in Reactor Scale Tokamaks, Arles, 244
GORMEZANO, C. (1991). Plasma Phys. and Cont. Fus., Berlin, Eur Conf. Abs. 15C, III, 393
GREENHOUGH, N. et al (1991). Fusion Engineering, San Diego, 126
HERSHKOWITZ, N. et al (1992). Boulder Workshop
HODGSON, E. (1991). J Nucl. Mat., 179, 383
HOSEA, J. et al (1990). Plasma Phys. and Contr. Nucl. Fus., Washington, I, 669
HOSEA, J.et al (1991). Radio Frequency Power in Plasmas, Charleston, 125
IDE, S. et al (1992). This conference.
IKEDA, Y.et al(1990). J Nucl. Mat., 176 & 177, 306

IKEDA, Y. et al (1991). Fusion Engineering, San Diego, 122
JACQUINOT, J.et al (1980). Fusion Technology, Oxford, 1101
JACQUINOT, J et al (1991). Plasma Phys. and Contr. Fus., 33, 1657
JACQUINOT, J.et al (1992). Accepted for publication in Phys.Fluids B
JAEGER, E.F. et al (1991). Radio Frequency Power in Plasmas, 159
JAEGER, E.F.et al (1992). Boulder Workshop
JT-60 Team (1990). Plasma Phys. and Contr. Nucl. Fus., Washington, 53
KAYE, A.S.et al (1987). Fusion Technology, 11, 1, 203
KAYE, A.S.et al (1988). Fusion Technology, Utrecht, 449
KAYE, A.S.et al (1992). Fus. Eng. and Design, to be published.
KIMURA, H. et al (1992). This conference
KOVALYOV, N.F. et al (1990). Workshop on Strong Microwaves in Plasmas, Suzdal.
LALLIA, P. (1974). RF Plasma Heating, Lubbok, C3-1
LEUTERER, F. et al (1991). Plasma Phys. and Contr. Fus. , 33, 3, 169-180
LITAUDON, X. et al (1992). To be published in Nucl. Fus.
LOBEL, R. et al (1990). Fusion Technology, London,1104
LONGINOV, A.V. (1989). ITER-IL-HD-7-9-S-1
MAJESKI, R.et al (1991). Radio Frequency Power in Plasmas, 322
MATSUMOTO, H. et al (1987). Nucl. Fus., 29, 1181
MOELLER, C.P. et al (1992). This conference
MOREAU, D. et al (1983). Radiation in Plasmas, Trieste, 331
MOREAU, D. (1987). Appl. of RF Power to Plasmas, Kissimee, 135
MOREAU, D. and Tore Supra Team (1992). Phys. Fluids, B4, 7, 2165
MYRA, J.R. (1990). Nucl. Fus., 30, 845
NGUYEN, T.K., MOREAU, D. (1982). Fusion Technology, Julich, 1381
NOTERDAEME, J-M.et al (1986). Contr. Fus. and Plasma Heating, Schliersee,137.
NOTERDAEME, J-M. (1991). Radio Frequency Power in Plasmas, Charleston, 71
NOTERDAEME, J-M. et al (1992). To be published in Fus. Eng. and Design.
OWENS, T.L.(1986). Contr. Fus. and Plasma Heating, Schliersee, 145
PARAIL, V. et al (1991). ITER Current Drive and Heating System, ITER Documentation Series No. 32
PERKINS, F.W. (1989). Nucl. Fus. 29, 4, 583
PETELIN, M.I,SUVOROV,E.V. (1989). SovJ.Tech.Phys (letters), 15, 23
PINSKER, R.I. et al (1991). Fusion Engineering, San Diego, 115
PINSKER, R. (1992). Boulder Workshop
REBUT, P-H. (1992). This conference.
REY, G. et al (1988). Fusion Technology, Utrecht, I, 514
SAIGUSA, M. (1991). Radio Frequency Power in Plasmas, Charleston, 193
SAKAMOTO, T et al (1986). IEEE Trans on Plasma Sci., PS-14, 4, 548
SEKI, M. et al (1990). Fusion Technology, London, II, 1060
STEINMETZ, K. et al (1987). Phys Rev Letters 58, 124
TONON, G. (1989). ITER Report ITER-IL-HD-5-9-E-2
TONON, G. (1990). ITER Report ITER-IL-HD-5-0-E-6
TUBBING, B,et al (1989). Nucl. Fus. 29, 1953
van der LAAN, J.G, AKIBA, M., HASSANEIN, A., SEKI, M.(1991). Paper 148, ISFNT-2, Karlsruhe
van OOST, G. et al (1992). This conference.
van NIEUWENHOVE, R. et al (1991). Nucl. Fus. 31, 9, 1770
WADE, T. et al (1991). Fusion Engineering, San Diego, 902
WALKER, C.I. et al (1988). Fusion Technology, Utrecht, 815
WALKER, C.I. et al (1992). Fusion Technology, Rome, to be published
WEGROVE, J-G.,PARAIL,V. (1991). FWCD in Reactor Scale Tokamaks, Arles, 402
WEDLER, H.et al (1992). Fus. Eng. and Design, to be published.
WILHELM, R. (1988). Fusion Technology, Utrecht, 167
YOSHIKAWA, S. et al (1965). Plasma Phys. and Contr. Fus. Research, Culham, 2, 925

Appendix I

THE JET TEAM

JET Joint Undertaking, Abingdon, Oxon, OX14 3EA, U.K.

J.M. Adams[1], B. Alper, H. Altmann, A. Andersen[14], P. Andrew, S.Ali-Arshad, W. Bailey, B. Balet, P. Barabaschi, Y. Baranov, P. Barker, R. Barnsley[2], M. Baronian, D.V. Bartlett, A.C. Bell, G. Benali, P. Bertoldi, E. Bertolini, V. Bhatnagar, A.J. Bickley, D. Bond, T. Bonicelli, S.J. Booth, G. Bosia, M. Botman, D. Boucher, P. Boucquey, M. Brandon, P. Breger, H. Brelen, W.J. Brewerton, H. Brinkschulte, T. Brown, M. Brusati, T. Budd, M. Bures, P. Burton, T. Businaro, P. Butcher, H. Buttgereit, C. Caldwell-Nichols, D.J. Campbell, D. Campling, P. Card, G. Celentano, C.D. Challis, A.V.Chankin[23], A. Cherubini, D. Chiron, J. Christiansen, P. Chuilon, R. Claesen, S. Clement, E. Clipsham, J.P. Coad, I.H. Coffey[24], A. Colton, M. Comiskey[4], S. Conroy, M. Cooke, S. Cooper, J.G. Cordey, W. Core, G. Corrigan, S. Corti, A.E. Costley, G. Cottrell, M. Cox[7], P. Crawley, O. Da Costa, N. Davies, S.J. Davies[7], H. de Blank, H. de Esch, L. de Kock, E. Deksnis, N. Deliyanakus, G.B. Denne-Hinnov, G. Deschamps, W.J. Dickson[19], K.J. Dietz, A. Dines, S.L. Dmitrenko, M. Dmitrieva[25], J. Dobbing, N. Dolgetta, S.E. Dorling, P.G. Doyle, D.F. Düchs, H. Duquenoy, A. Edwards, J. Ehrenberg, A. Ekedahl, T. Elevant[11], S.K. Erents[7], L.G. Eriksson, H. Fajemirokun[12], H. Falter, J. Freiling[15], C. Froger, P. Froissard, K. Fullard, M. Gadeberg, A. Galetsas, L. Galbiati, D. Gambier, M. Garribba, P. Gaze, R. Giannella, A. Gibson, R.D. Gill, A. Girard, A. Gondhalekar, D. Goodall[7], C. Gormezano, N.A. Gottardi, C. Gowers, B.J. Green, R. Haange, A. Haigh, C.J. Hancock, P.J. Harbour, N.C. Hawkes[7], N.P. Hawkes[1], P. Haynes[7], J.L. Hemmerich, T. Hender[7], J. Hoekzema, L. Horton, J. How, P.J. Howarth[5], M. Huart, T.P. Hughes[4], M. Huguet, F. Hurd, K. Ida[18], B. Ingram, M. Irving, J. Jacquinot, H. Jaeckel, J.F. Jaeger, G. Janeschitz, Z. Jankowicz[22], O.N. Jarvis, F. Jensen, E.M. Jones, L.P.D.F. Jones, T.T.C. Jones, J-F. Junger, F. Junique, A. Kaye, B.E. Keen, M. Keilhacker, W. Kerner, N.J. Kidd, R. Konig, A. Konstantellos, P. Kupschus, R. Lässer, J.R. Last, B. Laundy, L. Lauro-Taroni, K. Lawson[7], M. Lennholm, J.Lingertat[13], R.N. Litunovski, A. Loarte, R. Lobel, P. Lomas, M. Loughlin, C. Lowry, A.C. Maas[15], B. Macklin, C.F. Maggi[16], G. Magyar, V. Marchese, F. Marcus, J. Mart, D. Martin, E. Martin, R. Martin-Solis[8], P. Massmann, G. Matthews, H. McBryan, G. McCracken[7], P. Meriguet, P. Miele, S.F. Mills, P. Millward, E. Minardi[16], R. Mohanti[17], P.L. Mondino, A. Montvai[3], P. Morgan, H. Morsi, G. Murphy, F. Nave[27], S. Neudatchin[23], G. Newbert, M. Newman, P. Nielsen, P. Noll, W. Obert, D. O'Brien, J. O'Rourke, R. Ostrom, M. Ottaviani, S. Papastergiou, D. Pasini, B. Patel, A. Peacock, N. Peacock[7], R.J.M. Pearce, D. Pearson[12], J.F. Peng[26], R. Pepe de Silva, G. Perinic, C. Perry, M.A. Pick, J. Plancoulaine, J-P. Poffé, R. Pohlchen, F. Porcelli, L. Porte[19], R. Prentice, S. Puppin, S. Putvinskii[23], G. Radford[9], T. Raimondi, M.C. Ramos de Andrade, M. Rapisarda[29], P-H. Rebut, R. Reichle, S. Richards, E. Righi, F. Rimini, A. Rolfe, R.T. Ross, L. Rossi, R. Russ, H.C. Sack, G. Sadler, G. Saibene, J.L. Salanave, G. Sanazzaro, A. Santagiustina, R. Sartori, C. Sborchia, P. Schild, M. Schmid, G. Schmidt[6], H. Schroepf, B. Schunke, S.M. Scott, A. Sibley, R. Simonini, A.C.C. Sips, P. Smeulders, R. Smith, M. Stamp, P. Stangeby[20], D.F. Start, C.A. Steed, D. Stork, P.E. Stott, P. Stubberfield, D. Summers, H. Summers[19], L. Svensson, J.A. Tagle[21], A. Tanga, A. Taroni, C. Terella, A. Tesini, P.R. Thomas, E. Thompson, K. Thomsen, P. Trevalion, B. Tubbing, F. Tibone, H. van der Beken, G. Vlases, M. von Hellermann, T. Wade, C. Walker, D. Ward, M.L. Watkins, M.J. Watson, S. Weber[10], J. Wesson, T.J. Wijnands, J. Wilks, D. Wilson, T. Winkel, R. Wolf, D. Wong, C. Woodward, M. Wykes, I.D. Young, L. Zannelli, A. Zolfaghari[28], G. Zullo, W. Zwingmann.

PERMANENT ADDRESSES

1. UKAEA, Harwell, Didcot, Oxon, UK.
2. University of Leicester, Leicester, UK.
3. Central Research Institute for Physics, Budapest, Hungary.
4. University of Essex, Colchester, UK.
5. University of Birmingham, Birmingham, UK.
6. Princeton Plasma Physics Laboratory, New Jersey, USA.
7. UKAEA Culham Laboratory, Abingdon, Oxon, UK.
8. Universidad Complutense de Madrid, Spain.
9. Institute of Mathematics, University of Oxford, UK.
10. Freien Universität, Berlin, F.R.G.
11. Royal Institute of Technology, Stockholm, Sweden.
12. Imperial College, University of London, UK.
13. Max Planck Institut für Plasmaphysik, Garching, FRG.
14. Risø National Laboratory, Denmark.
15. FOM Instituut voor Plasmafysica, Nieuwegein, The Netherlands.
16. Dipartimento di Fisica, University of Milan, Milano, Italy.
17. North Carolina State University, Raleigh, NC, USA
18. National Institute for Fusion Science, Nagoya, Japan.
19. University of Strathclyde, 107 Rottenrow, Glasgow, UK.
20. Institute for Aerospace Studies, University of Toronto, Ontario, Canada.
21. CIEMAT, Madrid, Spain.
22. Institute for Nuclear Studies, Otwock-Swierk, Poland.
23. Kurchatov Institute of Atomic Energy, Moscow, USSR
24. Queens University, Belfast, UK.
25. Keldysh Institute of Applied Mathematics, Moscow, USSR.
26. Institute of Plasma Physics, Academica Sinica, Hefei, P. R. China.
27. LNETI, Savacem, Portugal.
28. Plasma Fusion Center, M.I.T., Boston, USA.
29. ENEA, Frascati, Italy.

At 1st July, 1992